Supporting Information
Conditional Dicer substrate formation
via shape and sequence transduction
with small conditional RNAs

Lisa M. Hochrein, Maayan Schwarzkopf, Mona Shahgholi, Peng Yin, and Niles A. Pierce

Contents

S1 Methods

S1.1 Oligonucleotide synthesis and preparation

Oligonucleotides were synthesized by Integrated DNA Technologies (IDT) and either HPLC purified by IDT or purified in the lab by denaturing polyacrylamide gel electrophoresis (PAGE) followed by ethanol precipitation. To establish correct stoichiometry for duplex scRNA reactants, the two strands were annealed (heating to 90 °C for 3 min followed by controlled cooling to 23 °C at 1 °C per min in a PCR block) and the duplex was isolated via native PAGE. Duplexes were then eluted in $1\times$ duplex buffer (100 mM potassium acetate, 20 mM HEPES, pH 7.5) overnight, filtered, and frozen (Mechanisms 2 and 4) or stored at 4 °C (Mechanism 3). scDNAs for Mechanism 5 were synthesized and PAGE purified in two pieces by IDT, then ligated to produce the full hairpin using T4 DNA ligase (New England Biolabs, catalog #M0202), followed by denaturing PAGE purification and ethanol precipitation. Prior to each reaction, all monomers were snap cooled (95 °C for 90 sec, 30 sec incubation on ice, and room temperature incubation of at least 30 min) and duplex dimers were either annealed (Mechanisms 2 and 4) or used without annealing after storage at 4 °C (Mechanism 3). For each mechanism, concentrations were estimated by measuring UV absorbance on a NanoDrop-8000 (Thermo Scientific) using extinction coefficients provided by IDT, and then scRNA or scDNA concentrations were corrected relative to the concentration of short target X_s by performing titration experiments (2 h reaction at 37 °C followed by native PAGE).

S1.2 Polyacrylamide gel electrophoresis

scRNA reactions were performed in $1\times$ duplex buffer (100 mM potassium acetate, 20 mM HEPES, pH 7.5) and scDNA reactions were performed in $1\times$ SPSC buffer (50 mM Na_2HPO_4, 0.5 M NaCl, pH 7.5). Reactants were incubated at 0.5 μM each for 2 h at 37 °C. The annealed reactions for stepping studies were run on a gel upon completion of the cooling protocol without further incubation. Gels were cast and run in $1\times$ TBE (Tris-Borate-EDTA). Native PAGE was performed using 20% native polyacrylamide gels run at 200 V for 8–10.5 h unless otherwise specified. Denaturing PAGE was performed using 15% denaturing polyacrylamide gels run at 500 V for 1.5 h unless otherwise specified. Each lane was loaded with a reaction volume corresponding to 2 pmol of the specified strands (4 pmol for mRNAs) in $1\times$ loading buffer. Gels were post-stained in $1\times$ SYBR Gold (Life Technologies, catalog #S-11494) for 10 min at room temperature and imaged using an FLA-5100 imaging system (Fuji Photo Film). For Dicer processing gels, 45 ng of siRNA markers (New England Biolabs, catalog #N2101) were used for native PAGE, or 60 ng of miRNA markers (New England Biolabs, catalog #N2102) were used for denaturing PAGE.

S1.3 Conditional radioactive shRNA transcription

For Mechanism 5, radioactive in vitro transcription was performed simultaneously with scDNA transduction using the T7-Scribe Standard RNA IVT kit (CELLSCRIPT, catalog #C-AS3107). 2 pmol of each scDNA were used for each 20 μL reaction. Transcription reactions were carried out as directed by the manufacturer with the following modification: 50 nmol of UTP and 3–4 μL of $[\alpha-^{32}P]$ UTP (10 mCi/mL, MP Biomedicals, catalog #0139313H01). Reactions were incubated for 3 h at 37 °C followed by 20 min of DNaseI treatment at 37 °C. The reaction volume was adjusted to 200 μL using RNase-free water and extracted using 1:1 (v/v) TE-saturated phenol/chloroform. Unincorporated NTPs were removed from the aqueous phase by NucAway spin columns (Life Technologies, catalog #AM10070) as directed by the manufacturer. Ethanol precipitation was done by incubation on ice for 15 min in 1:10 (v/v) of 3M sodium acetate and 2.5$\times$ (v/v) 95% EtOH. The RNA was pelleted at 4 °C and then washed with 70% EtOH. The pellet was dried and resuspended in $1\times$ duplex buffer. Counts were measured on an LS-5000TD Liquid Scintillation Counter (Beckman). siRNA markers (New England Biolabs, catalog #N2101) and miRNA markers (New England Biolabs, catalog #N2102) were 5′-end labeled with $[\gamma-^{32}P]$ ATP (10 mCi/mL, MP Biomedicals, catalog #0138101X01) using T4 polynucleotide kinase (New England Biolabs, catalog #M0201) to serve as size markers in radioactive gels. Unincorporated $[\gamma-^{32}P]$ ATP was removed by spin column chromatography using Illustra MicroSpin G-25 columns (GE Healthcare, catalog #27-5325-01) as directed by the manufacturer.

S1.4   Gel quantification

To characterize variability in scRNA and scDNA signal transduction performance for each mechanism, gels used for quantification of ON and OFF states were run on three separate days, preparing reactants each day as described above (see Sections S2.5, S3.5, S4.5, S5.5, S6.5). Multi Gauge software (Fuji Photo Film) was used to calculate the SYBR Gold intensity profile surrounding the band corresponding to the transduction product. Each intensity profile is displayed for $\pm$ 4mm of gel migration distance with the peak value centered at 0 (a smaller window than $\pm$ 4 mm was used for Mechanism 1 to avoid a nearby band). The intensity values are normalized so that the highest peak value for each gel is set to 1. The quantification percentages were calculated either using Multi Gauge (with auto-detection of signal and background) or using a Matlab script that subtracted the background, which was approximated by fitting a straight line to the intensity values in the last 0.5 mm at either end of the quantified window. The calculated values for ON and OFF states were normalized to the ON state for the short detection target X_s. After quantifying the gels shown in the main text six times each, the uncertainty in quantifying any given gel is estimated to be less than 0.5%. This gel quantification uncertainty is significantly smaller than the variability observed between the three independent reaction replicates for a given mechanism.

S1.5   In vitro Dicer processing

Dicer reactions were performed using the Recombinant Human Turbo Dicer Enzyme kit (Genlantis, catalog #T520002). For Mechanisms 1–4, the reactions were performed at 0.5 μM in 10 μL using enough Turbo Dicer to process approximately all of the final substrate after 2 h at 37 °C (0.5 units for Mechanisms 1–3 and 1 unit for Mechanism 4). Dicer, target and scRNAs were mixed simultaneously (i.e., the reactants were not pre-incubated with the target prior to addition of Dicer). siRNA production was verified by native PAGE. For Mechanism 5, the cognate shRNA Dicer substrate is a radio-labeled transcription product. Dicer reactions were performed following in vitro transcription. For a given Dicer processing gel, the same volume of transcription product was used for each reaction, determined so as to correspond to 20,000 cpm for the reaction containing short detection target X_s. Likewise, the same amount of Turbo Dicer was used for each reaction (1 unit of Dicer per 20,000 cpm in the X_s reaction). Radioactive gels were exposed overnight on an image plate (Fujifilm Type BAS-MS) and scanned using an FLA-5100 imaging system (Fuji Photo Film).

S1.6   mRNA in vitro transcription and preparation

The DsRed2, d2EGFP, and GAPDH mRNAs were generated by in vitro transcription. Plasmids were constructed, linearized, and transcribed as follows:

- **DsRed2.** The mRNA coding sequence was amplified from pDsRed2-C1 (Clontech, catalog #632407) and directionally cloned into the pTnT Vector (Promega, catalog #L5610) to construct plasmid pTnT-DsRed2. The plasmid was linearized using NotI (New England Biolabs, catalog #R0189) and in vitro transcribed for 2 to 4 h using the T7-Scribe Standard RNA IVT kit (CELLSCRIPT, catalog #C-AS3107).
- **d2EGFP.** The d2EGFP mRNA coding sequence was cloned from cells expressing d2EGFP (gift from Dr. C. Beisel; based on the pd2EGFP-1 (Clontech, catalog #6008-1) sequence) and cloned into the pGEM-T Easy Vector (Promega, catalog #A1360) to construct plasmid pGEM-T-Easy-d2EGFP. The plasmid was linearized using AatII (New England Biolabs, catalog #R0117) and in vitro transcribed for 2 to 4 h using the SP6-Scribe Standard RNA IVT kit (CELLSCRIPT, catalog #C-AS3106).
- **GAPDH.** The GAPDH mRNA coding sequence was cloned from HEK 293 cells and cloned into the pGEM-T Easy Vector (Promega, catalog #A1360) to construct plasmid pGEM-T-Easy-GAPDH. The plasmid was linearized using SphI-HF (New England Biolabs, catalog #R3182) and in vitro transcribed for 2 to 4 h using the SP6-Scribe Standard RNA IVT kit (CELLSCRIPT, catalog #C-AS3106).

Transcribed mRNA was purified using the RNeasy Protect Mini Kit (Qiagen, catalog #74124). Transcripts are expected to be slightly longer than the coding sequences listed below due to additional transcription at the start and termination sites. Relative to the standard DsRed2 mRNA sequence shown below, our in vitro transcribed

transcript contained the mutation `A220G`. Relative to the standard d2EGFP mRNA sequence shown below, our in vitro transcribed transcript contained the mutation `C480U`. mRNA concentrations were estimated based on UV absorbance on a NanoDrop-8000 (Thermo Scientific). Prior to each reaction, mRNAs were heated to 65 °C for 5 min and cooled at room temperature for a minimum of 30 min. mRNA targets (X, Y, or Z) were used at twice the estimated concentration of the short target X_s to account for uncertainties in concentration determination.

DsRed2 mRNA sequence
```
  1 AUGGCCUCCU CCGAGAACGU CAUCACCGAG UUCAUGCGCU UCAAGGUGCG CAUGGAGGGC
 61 ACCGUGAACG GCCACGAGUU CGAGAUCGAG GGCGAGGGCG AGGGCCGCCC CUACGAGGGC
121 CACAACACCG UGAAGCUGAA GGUGACCAAG GGCGGCCCCC UGCCCUUCGC CUGGGACAUC
181 CUGUCCCCCC AGUUCCAGUA CGGCUCCAAG GUGUACGUGA AGCACCCCGC CGACAUCCCC
241 GACUACAAGA AGCUGUCCUU CCCCGAGGGC UUCAAGUGGG AGCGCGUGAU GAACUUCGAG
301 GACGGCGGCG UGGCGACCGU GACCCAGGAC UCCUCCCUGC AGGACGGCUG CUUCAUCUAC
361 AAGGUGAAGU UCAUCGGCGU GAACUUCCCC UCCGACGGCC CCGUGAUGCA GAAGAAGACC
421 AUGGGCUGGG AGGCCUCCAC CGAGCGCCUG UACCCCCGCG ACGGCGUGCU GAAGGGCGAG
481 ACCCACAAGG CCCUGAAGCU GAAGGACGGC GGCCACUACC UGGUGGAGUU CAAGUCCAUC
541 UACAUGGCCA AGAAGCCCGU GCAGCUGCCC GGCUACUACU ACGUGGACGC CAAGCUGGAC
601 AUCACCUCCC ACAACGAGGA CUACACCAUC GUGGAGCAGU ACGAGCGCAC CGAGGGCCGC
661 CACCACCUGU UCCUGAGAUC UCGAGCUCAA GCUUCGAAUU CUGCAGUCGA CGGUACCGCG
721 GGCCCGGGAU CCACCGGAUC UAGAUAA
```

d2EGFP mRNA sequence
```
  1 AUGGUGAGCA AGGGCGAGGA GCUGUUCACC GGGGUGGUGC CCAUCCUGGU CGAGCUGGAC
 61 GGCGACGUAA ACGGCCACAA GUUCAGCGUG UCCGGCGAGG GCGAGGGCGA UGCCACCUAC
121 GGCAAGCUGA CCCUGAAGUU CAUCUGCACC ACCGGCAAGC UGCCCGUGCC CUGGCCCACC
181 CUCGUGACCA CCCUGACCUA CGGCGUGCAG UGCUUCAGCC GCUACCCCGA CCACAUGAAG
241 CAGCACGACU UCUUCAAGUC CGCCAUGCCC GAAGGCUACG UCCAGGAGCG CACCAUCUUC
301 UUCAAGGACG ACGGCAACUA CAAGACCCGC GCCGAGGUGA AGUUCGAGGG CGACACCCUG
361 GUGAACCGCA UCGAGCUGAA GGGCAUCGAC UUCAAGGAGG ACGGCAACAU CCUGGGGCAC
421 AAGCUGGAGU ACAACUACAA CAGCCACAAC GUCUAUAUCA UGGCCGACAA GCAGAAGAAC
481 GGCAUCAAGG UGAACUUCAA GAUCCGCCAC AACAUCGAGG ACGGCAGCGU GCAGCUCGCC
541 GACCACUACC AGCAGAACAC CCCCAUCGGC GACGGCCCCG UGCUGCUGCC CGACAACCAC
601 UACCUGAGCA CCCAGUCCGC CCUGAGCAAA GACCCCAACG AGAAGCGCGA UCACAUGGUC
661 CUGCUGGAGU UCGUGACCGC CGCCGGGAUC ACUCUCGGCA UGGACGAGCU GUACAAGAAG
721 CUUAGCCAUG GCUUCCCGCC GGAGGUGGAG GAGCAGGAUG AUGGCACGCU GCCCAUGUCU
781 UGUGCCCAGG AGAGCGGGAU GGACCGUCAC CCUGCAGCCU GUGCUUCUGC UAGGAUCAAU
841 GUGUAG
```

GAPDH mRNA sequence
```
  1 AUGGGGAAGG UGAAGGUCGG AGUCAACGGA UUUGGUCGUA UUGGGCGCCU GGUCACCAGG
 61 GCUGCUUUUA ACUCUGGUAA AGUGGAUAUU GUUGCCAUCA AUGACCCCUU CAUUGACCUC
121 AACUACAUGG UUUACAUGUU CCAAUAUGAU UCCACCCAUG GCAAAUUCCA UGGCACCGUC
181 AAGGCUGAGA ACGGGAAGCU UGUCAUCAAU GGAAAUCCCA UCACCAUCUU CCAGGAGCGA
241 GAUCCCUCCA AAAUCAAGUG GGGCGAUGCU GGCGCUGAGU ACGUCGUGGA GUCCACUGGC
301 GUCUUCACCA CCAUGGAGAA GGCUGGGGCU CAUUUGCAGG GGGGAGCCAA AAGGGUCAUC
361 AUCUCUGCCC CCUCUGCUGA UGCCCCCAUG UUCGUCAUGG GUGUGAACCA UGAGAAGUAU
421 GACAACAGCC UCAAGAUCAU CAGCAAUGCC UCCUGCACCA CCAACUGCUU AGCACCCCUG
481 GCCAAGGUCA UCCAUGACAA CUUUGGUAUC GUGGAAGGAC UCAUGACCAC AGUCCAUGCC
541 AUCACUGCCA CCCAGAAGAC UGUGGAUGGC CCCUCCGGGA AACUGUGGCG UGAUGGCCGC
601 GGGGCUCUCC AGAACAUCAU CCCUGCCUCU ACUGGCGCUG CCAAGGCUGU GGGCAAGGUC
661 AUCCCUGAGC UGAACGGGAA GCUCACUGGC AUGGCCUUCC GUGUCCCCAC UGCCAACGUG
```

```
721  UCAGUGGUGG ACCUGACCUG CCGUCUAGAA AAACCUGCCA AAUAUGAUGA CAUCAAGAAG
781  GUGGUGAAGC AGGCGUCGGA GGGCCCCCUC AAGGGCAUCC UGGGCUACAC UGAGCACCAG
841  GUGGUCUCCU CUGACUUCAA CAGCGACACC CACUCCUCCA CCUUUGACGC UGGGGCUGGC
901  AUUGCCCUCA ACGACCACUU UGUCAAGCUC AUUUCCUGGU AUGACAACGA AUUUGGCUAC
961  AGCAACAGGG UGGUGGACCU CAUGGCCCAC AUGGCCUCCA AGGAGUAA
```

S1.7   Computational sequence design

scRNA and scDNA sequences were designed using the multi-state sequence design feature of the NUPACK web application.[1] The sequences of the mRNA detection target X (DsRed2) and the mRNA silencing target Y (d2EGFP) were specified as external sequence constraints. For each reaction, the multi-state design problem was formulated in terms of a set of target secondary structures corresponding to key initial, intermediate, or final states in the reaction pathway (Table S1). Sequences were optimized to reduce the ensemble defect for each target secondary structure.[2,3] Based on additional computational stepping analyses performed using the Analysis page of the NUPACK web application (see Section S1.8), final sequence designs (see Sections S2.1, S3.1, S4.1, S5.1, S6.1) were selected from a list of promising candidate sequences returned by the designer. The subsequences of mRNA X and mRNA Y that were selected for each mechanism are shown in Table S1. Design calculations were performed using nearest-neighbor free energy parameters for RNA (Mechanisms 1–4) or DNA (Mechanism 5) at 37 °C in 1M Na$^+$.[4,5] Chemical modifications (2′OMe-RNA) were not accounted for in the physical model.

Each mechanism was designed assuming that Dicer processing would yield a canonical 21-nt siRNA. Hence, sequence domains were dimensioned to ensure that this 21-nt siRNA addressing silencing target mRNA Y would have no sequence dependence on detection target mRNA X. In our mass spectrometry studies, we found that Recombinant Human Turbo Dicer (Genlantis, catalog #T520002) typically produces canonical 21–23-nt siRNAs. As a result, some siRNAs have a small unintended sequence dependence on mRNA X at one end. Future scRNA and scDNA designs should ensure sequence independence for at least a 23-nt siRNA product of Dicer processing.

Mechanism	Target structures	mRNA detection target X DsRed2 subsequence	mRNA silencing target Y d2EGFP subsequence
1	X$_s$, A, B, C, X$_s$·A, X$_s$·A·B	592–618	252–271
2	X$_s$, A, B, C, A·B, A·B·C, X$_s$·A, B·C	598–615	542–562
3	X$_s$, A, B, A·B, X$_s$·A	277–305	137–157
4	X$_s$, A·B, C·D, B·C	9–46	70–92
5	X$_s$, A, B	–	240–258

Table S1. Multi-state sequence design. For each mechanism, the objective function was formulated in terms of multiple target secondary structures with base-pairing states depicted in the mechanism schematics of Figs 2–6. For Mechanism 2, the target secondary structure for A was single-stranded, and the target secondary structure for 'trimer' A·B·C was comprised of duplex A·B and hairpin C. For Mechanism 3, the target secondary structure for A was single-stranded. Subsequences of mRNA detection target X and mRNA silencing target Y selected during the design process (for Mechanism 5, the sequence of the detection target was not constrained).

S1.8   Computational and experimental stepping analyses.

Equilibrium test tube calculations (see Sections S2.2, S3.2, S4.2, S5.2, S6.2) were performed using the analysis feature of the NUPACK web application[1] to step through the molecular assembly and disassembly operations for each mechanism (depicted in the mechanism schematics of Figs 2–6). These calculations were used to check that the desired reactants, intermediates, and products were predicted to form with high yield in test tubes containing different subsets of strands. Typically, we observed that sequence domains that were intended to be completely unstructured were predicted to have some degree of base pairing at equilibrium. These imperfections reflect the challenge of designing scRNA and scDNA hybridization cascades using sequences that are predominantly constrained to be

drawn from mRNAs X and Y. Analysis calculations were performed using nearest-neighbor free energy parameters for RNA (Mechanisms 1–4) or DNA (Mechanism 5) at 37 °C in 1M Na$^+$.[4,5] Chemical modifications (2′OMe-RNA) were not accounted for in the physical model. Similar mechanism stepping analyses were then performed experimentally to verify that the desired assembly and disassembly operations occurred with high yield (see Sections S2.3, S3.3, S4.3, S5.3, S6.3). Finally, these stepping analyses were repeated in the context of Dicer to verify that only the final product of signal transduction, and not the reactants or intermediates, were efficiently processed by Dicer (see Sections S2.4, S3.4, S4.4, S5.4, S6.4).

S1.9 Interpretation of annealed reactions

In the stepping experiments, we include both isothermal and annealed reactions for each step (see Sections S2.3, S3.3, S4.3, S5.3, S6.3). In structural nucleic acid nanotechnology, annealing (heating followed by slow cooling) is often relied on to relax systems to equilibrium.[6] However, for nucleic acid self-assembly systems that involve metastable hairpin monomers, annealing can dramatically fail to relax systems to equilibrium.[7,8] During the cooling phase of the anneal, intramolecular base pairs become favorable at higher temperatures than intermolecular base pairs, allowing hairpins to close before it becomes energetically favorable to interact with other molecules. If the hairpin is designed to be metastable, closure of the hairpin resets the kinetic trap and and inhibits relaxation to equilibrium. Hence, care should be used in interpreting annealed reactions involving hairpins or other strands with strong internal secondary structure.

S1.10 Mass spectrometry

Liquid chromatography-mass spectrometry (LC-MS) was used to measure the masses of Dicer cleavage products. Our objective was to determine whether bands that migrate with approximately the mobility of siRNAs were in fact siRNAs. Masses were determined for specific bands from native PAGE experiments (typically corresponding to either siRNAs or corresponding waste products) as well as for full reactions (i.e., without gel purification). Dicer processing, native PAGE and gel imaging were performed as described above with a 20× scaled-up Dicer reaction. Gel bands of interest were each excised from the gel, crushed, and soaked in H$_2$O. Samples were heated to 65° C for 5 min followed by an overnight incubation at room temperature. Samples were filtered by Nanosep MF 0.45μM (Pall Life Sciences, catalog #ODM45C35) and concentrated using Oligo Clean and Concentrator (Zymo Research, catalog #D4060) as directed by the manufacturer. For Mechanisms 1–3, average masses were determined by electrospray ionization time-of-flight (ESI-TOF) LC-MS with an estimated mass accuracy of ±0.02%. For Mechanisms 4 and 5, monoisotopic masses were determined by Novatia (New Jersey, USA) using high resolution ion trap LC-MS (LTQ-Orbitrap) with an estimated mass accuracy of ±0.0005%.

Sequence assignments for measured masses were made as follows:

- Step 1: For the sequences in a given Dicer substrate, we compiled a list of all possible subsequences consistent with a measured mass. At a Dicer cut site, the mass of the 3′ product was calculated with a 5′ phosphate group and the mass of the 5′ product was calculated with a 3′ hydroxyl group.[9] Chemical modifications (2′OMe-RNA) were taken into consideration for mass calculations. For Mechanisms 1–3, a Matlab script was used to identify all candidate subsequences within ±0.1% of the measured mass. For Mechanisms 4 and 5, the list of candidate subsequences was provided by Novatia. For measured masses with only one candidate subsequence, we assigned that sequence.

- Step 2: For measured masses with more than one candidate subsequence, each subsequence implies a different cut site. For a given cut site, we checked to see if the corresponding fragments were amongst the candidate subsequences for measured masses. By conservation of mass, sequences were assigned to masses if only one set of self-consistent fragments was identified. For example, two fragments are self-consistent if together they produce the full sequence. This approach could not be used for cut sites leading to fragments shorter than ≈10 nt as these were removed during sample preparation (Oligo Clean and Concentrator).

- Step 3: For measured masses with more than one candidate subsequence where self-consistent fragments of a given strand could not be identified (e.g., if one of the fragments was too short), we then checked to see if the

2-nt 3′-offset cut site of the hybridization partner within the substrate would lead to self-consistent fragments of the hybridization partner. By conservation of mass for the hybridization partner, and based on the known propensity for Dicer to produce products with 2-nt 3′ overhangs,[9] sequences were assigned to masses if only one set of self-consistent assignments was identified.

These steps were sufficient to uniquely assign sequences to the Dicer products shown in Sections S2.6, S3.6, S4.6, S5.6, and S6.6.

For ESI-TOF LC-MS analyses, dried samples were dissolved in 5-7 μL of deionized water. Typically, 4 μL were analyzed. Liquid chromatographic separations were performed using a Waters Acquity UPLC OST column (1.0 × 50 mm OST column, 1.7μm), and a Waters Acquity UPLC System. LC conditions were:

Column temperature:	60 °C	
Flow rate :	0.13 mL/min	
Mobile phase A:	16 mM triethylamine (TEA) / 400 mM hexafluoroisopropanol (HFIP)/ 2% MeOH, pH 8	
Mobile phase B:	16 mM TEA / 400 mM HFIP/ 60% MeOH, pH 8	
Linear gradient:	Time (min)	B (%)
	0	15
	20	65
	22	100
	24	100
	25	15
	30	15

The Acquity UPLC System was interfaced with a Waters LCT Premier XE ESI-TOF mass spectrometer. ESI conditions were:

Polarity:	ES(-)
Analyzer:	V mode
Capillary voltage:	2600 V
Desolvation temperature:	450 °C
Source temperature:	150 °C
Desolvation gas flow:	700 L/hr
Cone gas glow:	30 L/hr

Mass spectra were acquired from m/z 700 to m/z 1950 and deconvoluted using the Waters MaxEnt1 deconvolution algorithm.

S2 Mechanism 1: Conditional catalytic DsiRNA formation using metastable scRNAs

S2.1 Sequences

Strand	Domains	Sequence
X_s	s1-a-b-c-d-s2	5′-GGCAAGCUGGACAUCACCUCCCACAACGAGGAC-3′
A	b-c-v-w-x-y-e-d*-c*-b*-a*	5′-UCACCUCCCACAACGCUUCAAGUCCGCCAUCUCUCGUUGUGGGAGGUGAUGUCCAGCUU-3′
B	w-x-y-z-c-y*-x*-w*-v*-c*	5′-UCAAGUCCGCCAUGCCCGCAACGAUGGCGGACUUGAAGCGUUG-3′
C	y-z-c-v-w-x-y-c*-z*-y*-x*-w*-v*	5′-CGCCAUGCCCGCAACGCUUCAAGUCCGCCAUCGUUGCGGGCAUGGCGGACUUGAAG-3′

Table S2. Sequences for Mechanism 1. Sequences constrained by DsRed2 (mRNA detection target X) are shown in red. Sequences constrained by d2EGFP (mRNA silencing target Y) are shown in green. Unconstrained sequences are shown in black. Underlined nucleotides are 2′OMe-RNA; all other nucleotides are RNA. Domain lengths: |a|=10, |b|=10, |c|=5, |d|=2, |e|=2, |s1|= 3, |s2|= 3, |v|=2, |w|=5, |x|=2, |y|=6, |z|=5. To allow for better gel separation of the various reactants, intermediates, and products using native PAGE, the length of X_s was increased (by adding 3 nt to the 3′ end and 3 nt to the 5′ end). As an unintended consequence of shortening a sequence domain in hairpin C, the 5′-most nucleotide of the cognate siRNA guide strand is not complementary to the d2EGFP silencing target. Mutations at the 5′ end of the guide strand are well-tolerated,[10] and for human Ago2, similar silencing activities are observed with either the correct or mutated base at the 5′ end.[11] We therefore allowed this mismatch to remain in the design. However, in future designs, the length of the 'z' domain should be increased by 1 nt to avoid introducing a mismatch between the guide strand and its silencing target. Furthermore, based on our mass spectrometry studies demonstrating that Recombinant Human Turbo Dicer (Genlantis, catalog #T520002) typically yields canonical 21–23-nt siRNAs, future designs should ensure sequence independence for at least a 23-nt siRNA product of Dicer processing (see Section S1.7).

S2.2 Computational stepping analysis
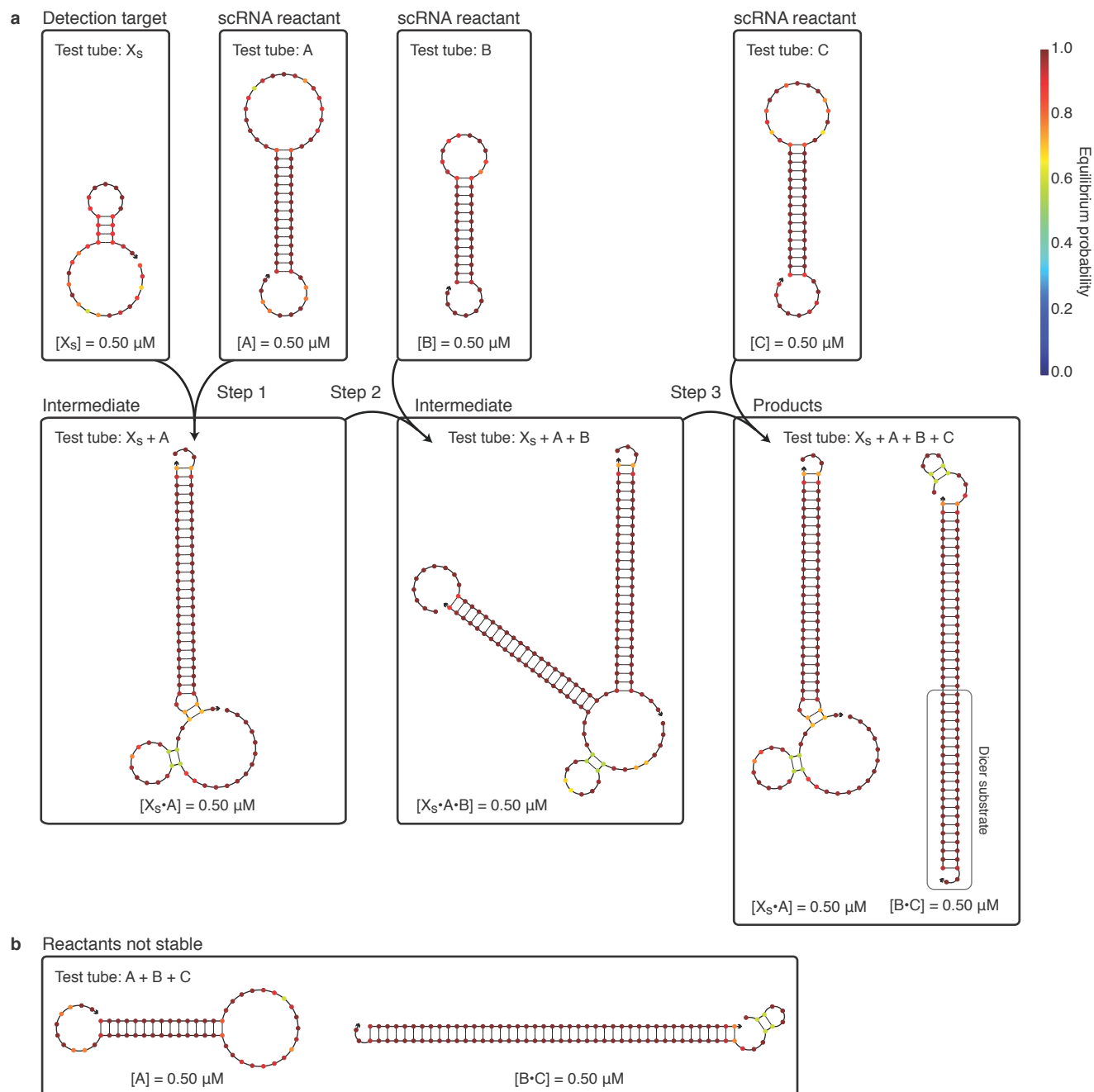
Figure S1. Computational stepping analysis for Mechanism 1. (a) Equilibrium test tube calculations showing the predicted concentrations and base-pairing properties of reactants, intermediates, and products. The short RNA detection target X_s is predicted to have some internal base pairing on average at equilibrium. Reactants, intermediates, and products are predicted to form with quantitative yield. In the intermediates, domains that are intended to be single-stranded are predicted to contain some weak base pairing on average at equilibrium. (b) Equilibrium test tube calculation predicting that scRNAs B and C are metastable, not stable. Placing A, B, and C together in a test tube leads predominantly to monomer hairpin A and duplex dimer B·C at equilibrium, demonstrating that B and C are not stable. (a,b) Each box represents a test tube containing the strands listed at the top at 0.5 μM each. For each test tube, thermodynamic analysis at 37 °C yields the equilibrium concentrations and base-pairing ensemble properties for all complexes containing up to four strands. Each complex predicted to form with appreciable concentration at equilibrium is depicted by its minimum free energy structure, with each nucleotide shaded by the probability that it adopts the depicted base-pairing state at equilibrium. The predicted equilibrium concentration is noted below each complex.

S2.3   Mechanism stepping gel
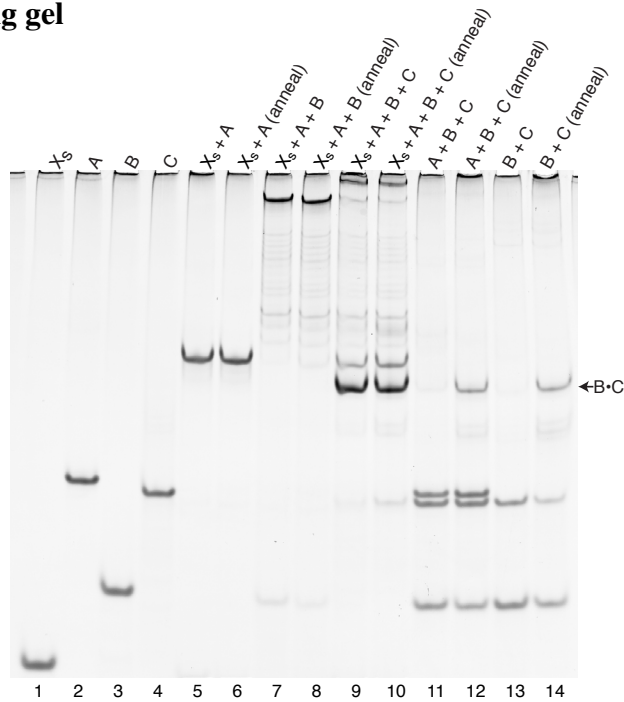
Figure S2. Stepping gel for Mechanism 1. Native PAGE demonstrating the assembly and disassembly operations in Figure 2a. Short RNA detection target: X_s (lane 1). scRNA reactants: A, B and C (lanes 2–4). Step 1: X_s and A interact to form catalyst $X_s \cdot A$ (lane 5). Step 1 + Step 2: X_s, A and B interact to form intermediate $X_s \cdot A \cdot B$ (lane 7). Step 1 + Step 2 + Step 3 (ON state): X_s, A, B and C interact to form catalyst $X_s \cdot A$, intermediate $X_s \cdot A \cdot B \cdot C$, and Dicer substrate B·C (lane 9). OFF state: A, B and C co-exist metastably, yielding minimal production of B·C (lane 11). Annealing A, B and C leads to increased production of B·C (lane 12). Hairpins B and C co-exist metastably, yielding minimal production of B·C (lane 13). Annealing B and C leads to increased production of B·C (lane 14). See Section S7 for an assessment of reactant metastability vs stability.

S2.4   Dicer processing stepping gel
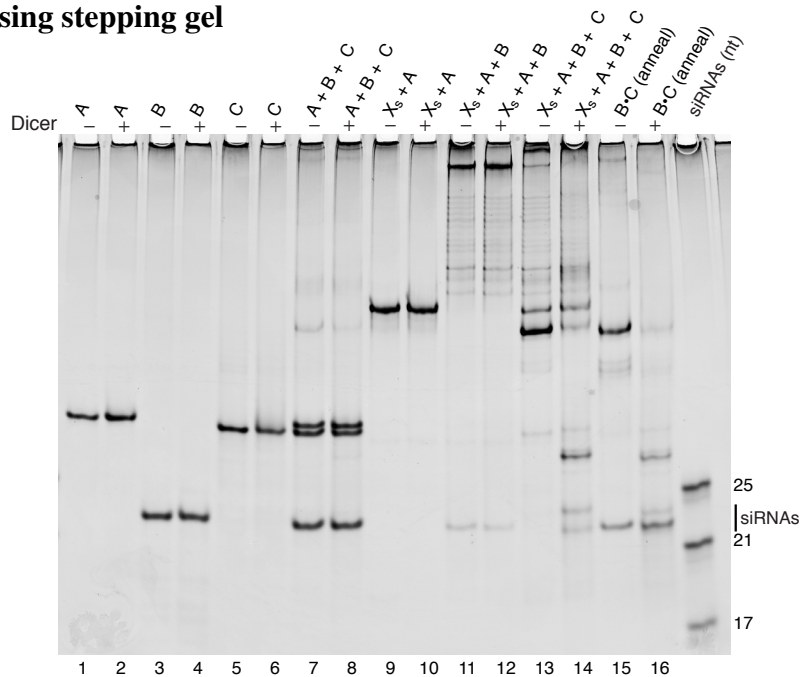
Figure S3. Dicer processing stepping gel for Mechanism 1. Native PAGE demonstrating each signal transduction step in Dicer reaction conditions in the absence/presence of Dicer (-/+ lanes). Only the final product B·C is efficiently processed by Dicer, yielding siRNAs (compare lanes 13 and 14).

S2.5 Quantification of conditional catalytic Dicer substrate formation
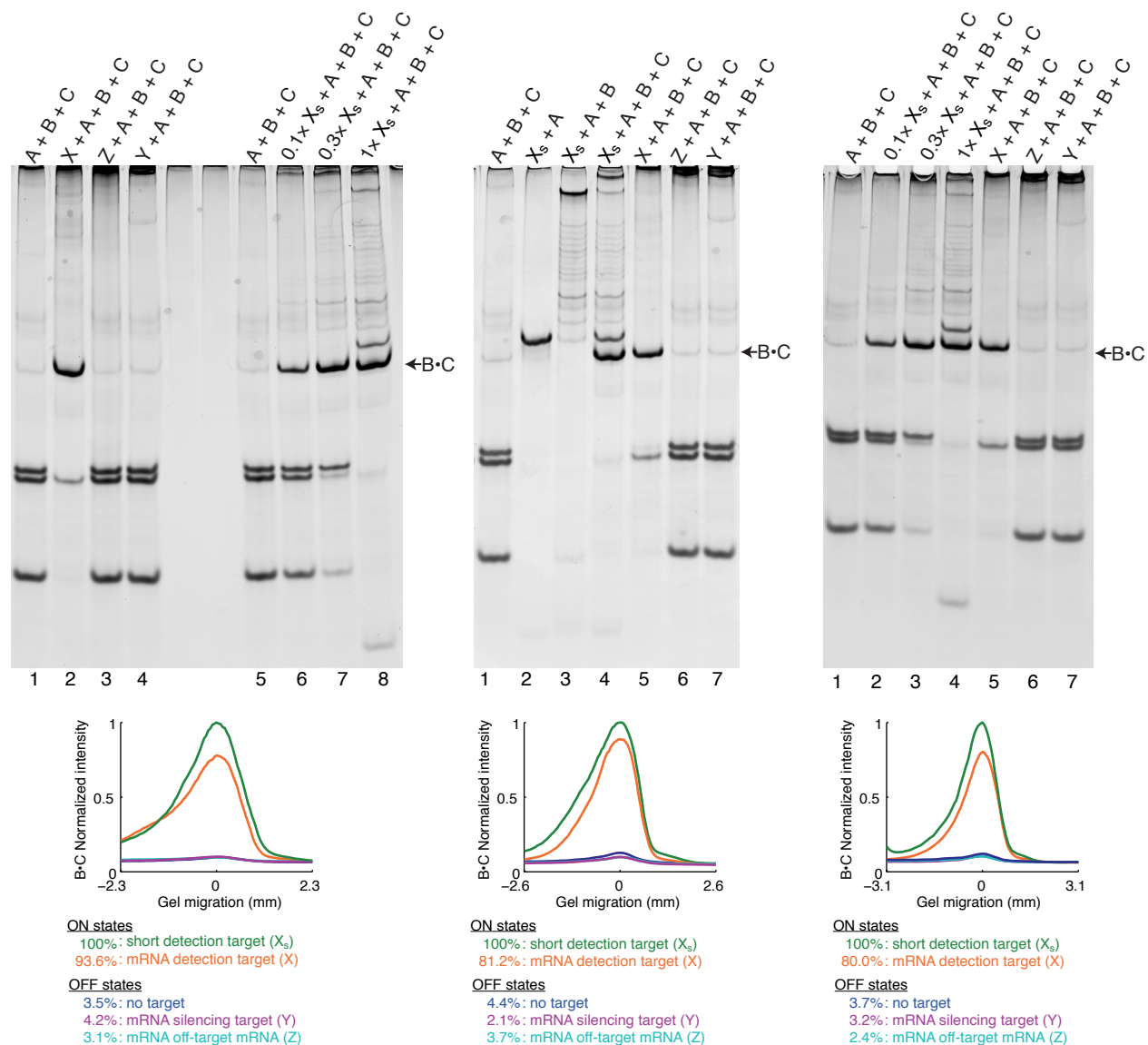
Figure S4. Quantification of conditional Dicer substrate formation for Mechanism 1. Three independent experiments were used to characterize the variability in the OFF/ON conditional response in production of Dicer substrate. OFF states: no target, mRNA silencing target Y, mRNA off-target Z. ON states: short RNA detection target X_s, mRNA detection target X. All values are normalized relative to the amount of Dicer substrate produced using X_s.
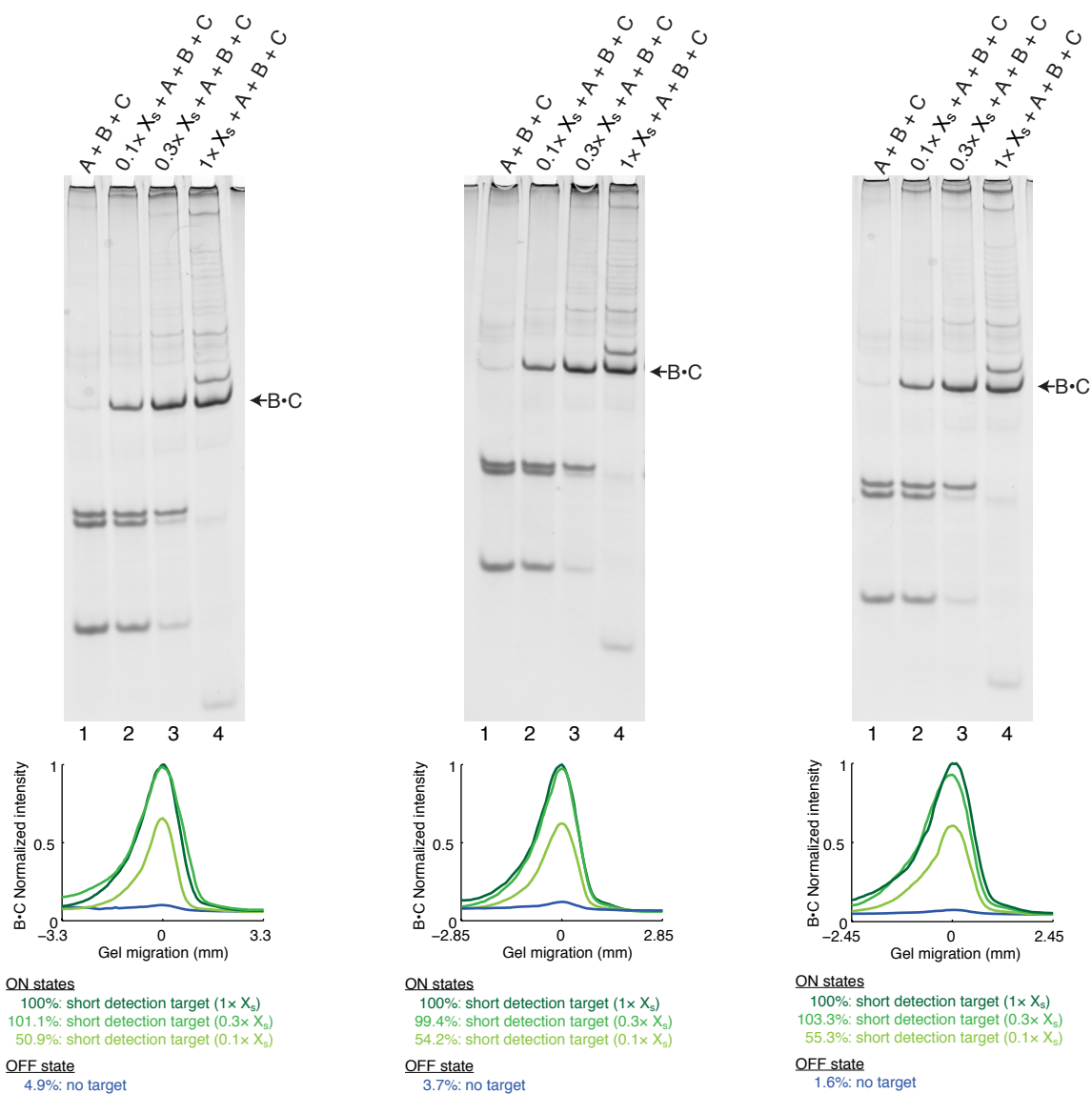
Figure S5. Quantification of catalytic Dicer substrate formation for Mechanism 1. Three independent experiments were used to characterize the variability in the catalytic production of Dicer substrate. OFF state: no target. ON states: short RNA detection target X_s at three concentrations ($0.1\times$, $0.3\times$, $1\times$) relative to the scRNA reactants. All values are normalized relative to the amount of Dicer substrate produced using $1\times X_s$.

S2.6 Identification of Dicer products by mass spectrometry

a

Dicer substrate						
scRNA						
C	GAAGUUCAGGCGGUACGGGCGUUGCUACGCGCCUGAACUUCGCAACGCCCGUACCGC					
B	UCAAGUCCGCCAUGCCCGCAACGAUGGGCGGACUUGAAGCGUUG					

Dicer products	Length (nt)	Predicted mass (Da)	Measured mass (Da)	Number of measurements			
				Gel band			Full reaction
				I	II	III	
23-nt siRNA / Waste							
GAAGUUCAGGCGGUACGGGCGUUp	23	7538.5	7537.8 ± 0.5	–	5	–	2
UCAAGUCCGCCAUGCCCGCAACG	23	7280.4	7280.0 ± 0.5	–	5	4	2
GCUACCGCCUGAACUUCGCAACGCCCGUACCGC	33	10690.8	10690.3 ± 0.6	5	–	–	2
pAUGGCGGACUUGAAGCGUUG	20	6613.0	6612.5 ± 0.2	5	–	–	2
21-nt siRNA trimmed from 23-nt siRNA / Waste							
AGUUCAGGCGGUACGGGCGUUp	21	6864.1	6863.5 ± 0.3	–	–	3	1
pAAGUCCGCCAUGCCCGCAACG	21	6749.1	6748.8 ± 0.6	–	2	3	2
GCUACCGCCUGAACUUCGCAACGCCCGUACCGC	33	10690.8	10690.3 ± 0.6	5	–	–	2
pAUGGCGGACUUGAAGCGUUG	20	6613.0	6612.5 ± 0.2	5	–	–	2

Table S3. Dicer products for Mechanism 1 identified by mass spectrometry. (a) Predicted and measured average masses for Dicer cleavage products. Canonical 21- and 23-nt siRNAs were identified, as were waste products corresponding to the non-siRNA portion of the substrate. The 21-nt siRNA appears to have been trimmed from the 23-nt siRNA. Masses were determined for specific gel bands (I, II, III) and for the full reaction. For each mass, the mean and standard deviation were calculated using all measurements. 5′ phosphate group is denoted 'p' and strand polarity is indicated by an arrowhead at the 3′ end. See Table S2 for 2′OMe-RNA chemical modifications. (b) Native PAGE illustrating the approximate migration of gel bands (I, II, III) that were isolated for mass spectrometry. See Supplementary Section S1.10 for methods.

S3 Mechanism 2: Conditional DsiRNA formation using stable scRNAs

S3.1 Sequences

Strand	Domains	Sequence
X_s	s1-a-b-c-s2	5′-CUGGACAUCACCUCCCACAACGAGGACUA-3′
A	c*-b*-a*-z*-y*	5′-GUUGUGGGAGGUGAUGUCGGGUGUU-3′
B	x-y-z-a-b	5′-CACUACCAGCAGAACACCCGACAUCACCU-3′
C	w-x-y-s-a*-z*-y*-x*-w*	5′-ACCACUACCAGCAGAACAAGGUAGAUGUCGGGUGUUCUGCUGGUAGUGGU-3′

Table S4. Sequences for Mechanism 2. Sequences constrained by DsRed2 (mRNA detection target X) are shown in red. Sequences constrained by d2EGFP (mRNA silencing target Y) are shown in green. Unconstrained sequences are shown in black. Underlined nucleotides are 2′OMe-RNA; all other nucleotides are RNA. Domain lengths: |a|=6, |b|=4, |c|=8, |s|=5, |s1|=3, |s2|=8, |w|=2, |x|=12, |y|=4, |z|=3. To allow for better gel separation of the various reactants, intermediates, and products using native PAGE, the length of X_s was increased (by adding 3 nt to the 3′ end and 8 nt to the 5′ end) and 5 nt were inserted in the loop of C.

S3.2 Computational stepping analysis
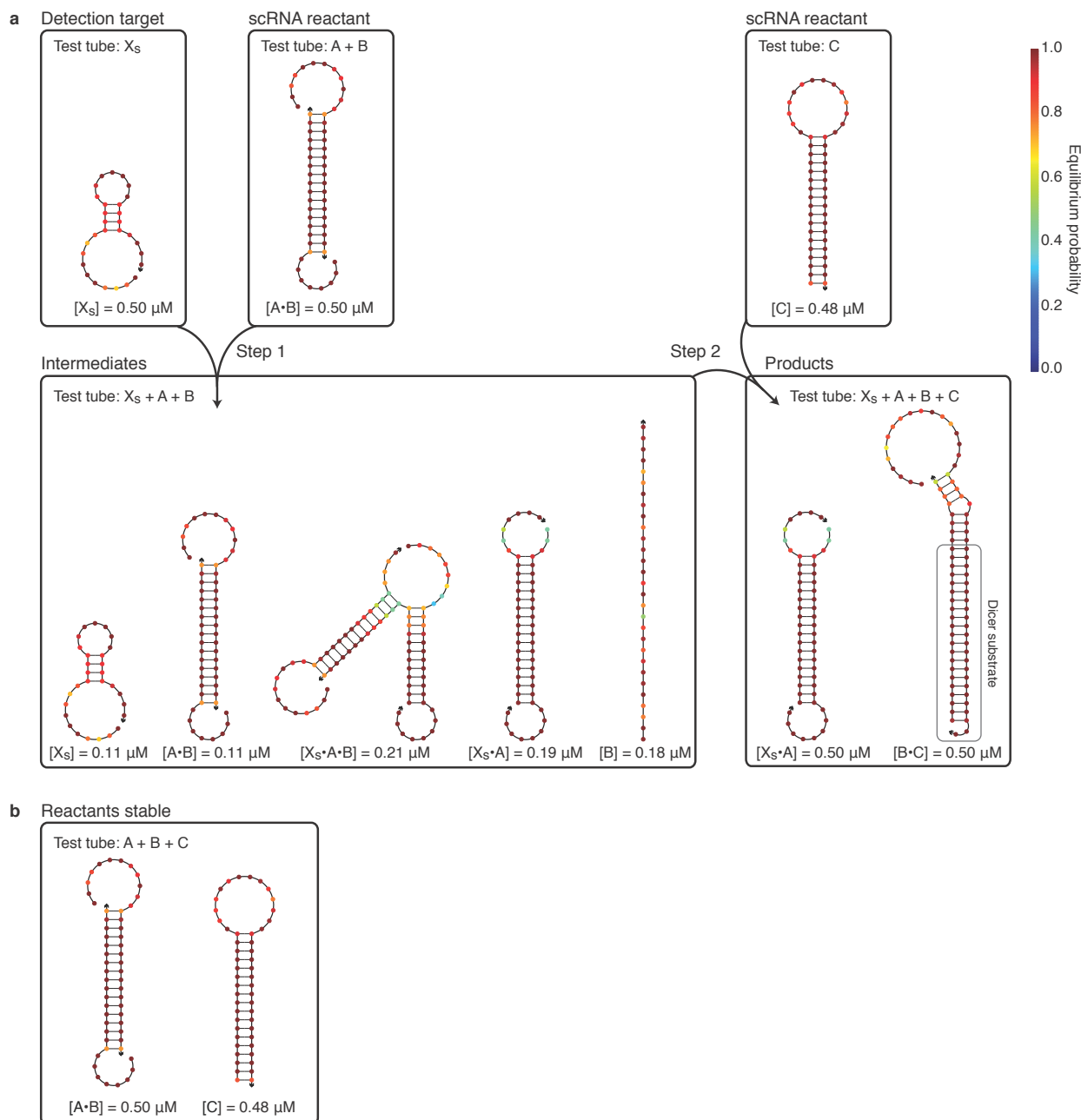
Figure S6. Computational stepping analysis for Mechanism 2. (a) Equilibrium test tube calculations showing the predicted concentrations and base-pairing properties of reactants, intermediates, and products. The short RNA detection target X_s is predicted to have some internal base pairing on average at equilibrium. Reactants are predicted to form with near-quantitative yield. Step 1 yields several complexes with appreciable yield at equilibrium. The desired intermediates are $X_s \cdot A$ and B. As expected, these exist in equilibrium with the intermediate $X_s \cdot A \cdot B$ since this mechanism relies on spontaneous dissociation of B from $X_s \cdot A$. Finally, some of the target X_s and scRNA A·B are unreacted, in part due to the internal secondary structure in X_s. After Step 2, the products form with quantitative yield, with C driving the reaction to completion. (b) Equilibrium test tube calculation predicting that scRNAs A·B and C are stable, not metastable. Placing A, B, and C together in a test tube leads predominantly to duplex dimer A·B and hairpin monomer C at equilibrium, demonstrating that reactants A·B and C are stable. (a,b) Each box represents a test tube containing the strands listed at the top at 0.5 μM each. For each test tube, thermodynamic analysis at 37 °C yields the equilibrium concentrations and base-pairing ensemble properties for all complexes containing up to four strands. Each complex predicted to form with appreciable concentration at equilibrium is depicted by its minimum free energy structure, with each nucleotide shaded by the probability that it adopts the depicted base-pairing state at equilibrium. The predicted equilibrium concentration is noted below each complex.

S3.3 Mechanism stepping gel
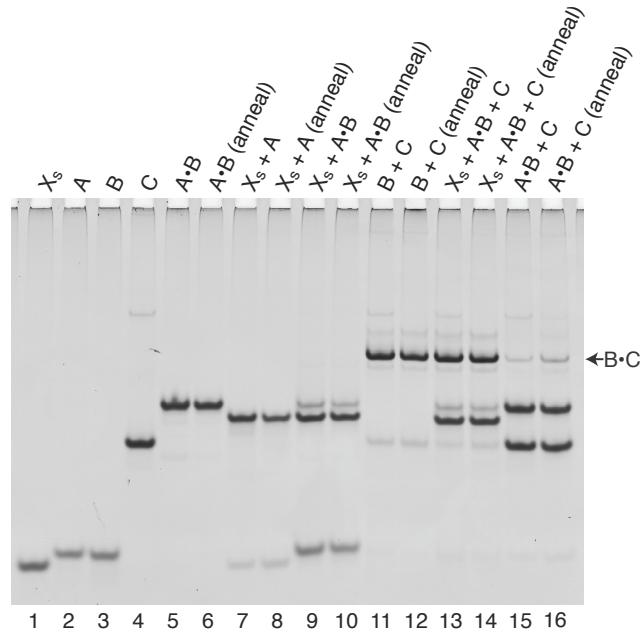
Figure S7. Stepping gel for Mechanism 2. Native PAGE demonstrating the assembly and disassembly operations in Figure 3a. Short RNA detection target: X_s (lane 1). scRNA reactants: C and A·B (lanes 4 and 5). Step 1: X_s and A·B interact to form product X_s·A and intermediate B (lane 9). Step 2: B and C interact to form product B·C (lane 11). Step 1 + Step 2 (ON state): X_s, A·B, and C interact to form products X_s·A and B·C (lane 13). OFF state: A·B and C co-exist stably, yielding minimal production of A and B·C (lane 15). Annealing A·B and C yields slightly higher production of A and B·C (lane 16). See Section S7 for an assessment of reactant metastability vs stability.

S3.4 Dicer processing stepping gel
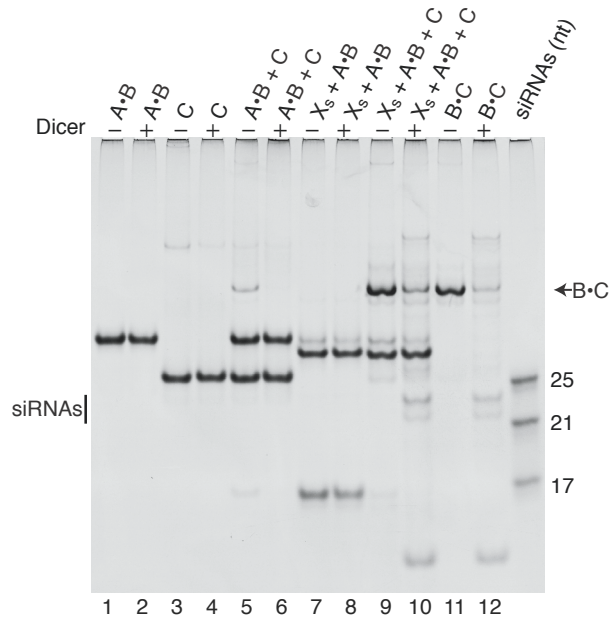
Figure S8. Dicer processing stepping gel for Mechanism 2. Native PAGE demonstrating each signal transduction step in Dicer reaction conditions in the absence/presence of Dicer (-/+ lanes). Only the final product B·C is efficiently processed by Dicer, yielding siRNAs (compare lanes 9 and 10).

S3.5 Quantification of conditional Dicer substrate formation
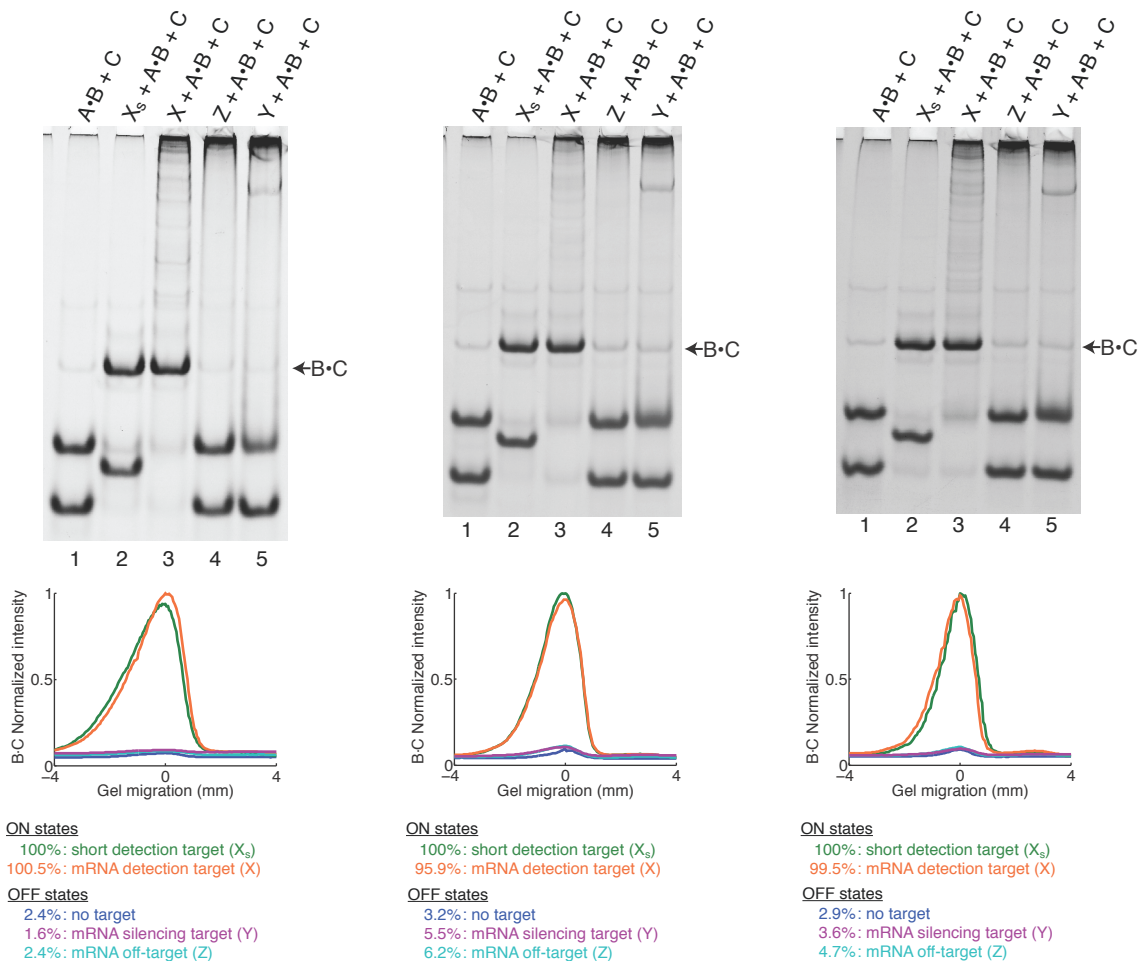
Figure S9. Quantification of conditional Dicer substrate formation for Mechanism 2. Three independent experiments were used to characterize the variability in the OFF/ON conditional response in production of Dicer substrate. OFF states: no target, mRNA silencing target Y, mRNA off-target Z. ON states: short RNA detection target X_s, mRNA detection target X. All values are normalized relative to the amount of Dicer substrate produced using X_s.

S3.6 Identification of Dicer products by mass spectrometry

a

Dicer substrate

scRNA

C: UGGUGAUGGUCGUCUUGUGUGGCUGUAGAUGGAACAAGACGACCAUCACCA

B: CACUACCAGCAGAAACACCCGACAUCACCU

Dicer products

Dicer products	Length (nt)	Predicted mass (Da)	Measured mass (Da)	Number of measurements			
				Gel band			Full reaction
				I	II	III	
23-nt siRNA							
Waste							
UGGUGAUGGUCGUCUUGUGUGGCUp	23	7470.3	7469.8 ± 0.4	2	2	–	1
CACUACCAGCAGAAACACCCGACA	23	7294.8	7294.6 ± 0.8	1	–	–	1
GUAGAUGGAACAAGACGACCAUCACCA	27	9050.0	9049.4 ± 0.8	–	–	1	1
22-nt siRNA							
Waste							
UGGUGAUGGUCGUCUUGUGUGGGCp	22	7164.2	7163.5 ± 0.8	2	2	–	1
CACUACCAGCAGAAACACCCGAC	22	6965.6	6964.6 ± 0.1	1	3	–	–
UGUAGAUGGAACAAGACGACCAUCACCA	28	9356.2	9355.7 ± 0.1	–	–	1	1
21-nt siRNA trimmed from 23-nt siRNA							
Waste							
GUGAUGGUCGUCUUGUGUGGGCUp	21	6819.0	6818.8 ± 0.1	1	3	–	1
pCUACCAGCAGAAACACCCGACA	21	6740.1	6739.8 ± 0.5	2	3	–	1
GUAGAUGGAACAAGACGACCAUCACCA	27	9050.0	9049.4 ± 0.8	–	–	1	1

b

siRNAs (nt)

Target: – – – –
Dicer: – + – +
OFF | ON
Xs | Xs Xs
– | + –

B•C
Xs•A
25
siRNAs
21
17

A•B–
C–

I II III
1 2 3 4

Table S5. Dicer products for Mechanism 2 identified by mass spectrometry. (a) Predicted and measured average masses for Dicer cleavage products. Canonical 21–23-nt siRNAs were identified, as were waste products corresponding to the non-siRNA portion of the substrate (only the waste from strand C was identified as the waste from strand B was too short to be retained during sample purification). The 21-nt siRNA appears to have been trimmed from the 23-nt siRNA. Masses were determined for specific gel bands (I, II, III) and for the full reaction. For each mass, the mean and standard deviation were calculated using all measurements. 5′ phosphate group is denoted 'p' and strand polarity is indicated by an arrowhead at the 3′ end. See Table S4 for 2′OMe-RNA chemical modifications. (b) Native PAGE illustrating the approximate migration of gel bands (I, II, III) that were isolated for mass spectrometry. See Supplementary Section S1.10 for methods.

S4 Mechanism 3: Conditional shRNA formation using a single stable scRNA

S4.1 Sequences

Strand	Domains	Sequence
X_s	a-b-c	5′–UGGGAGCGCGUGAUGAACUUCGAGGACGG–3′
A	z-c*-b*-a*	5′–UUCAUCUGCACCACCGGCACCGUCCUCGAAGUUCAUCACGCGCUCCCA–3′
B	z-c*-b-c-z*-y*	5′–UUCAUCUGCACCACCGGCACCGAUGAACUUCGAGGACGGUGCCGGUGGUGCAGAUGAACU–3′

Table S6. Sequences for Mechanism 3. Sequences constrained by DsRed2 (mRNA detection target X) are shown in red. Sequences constrained by d2EGFP (mRNA silencing target Y) are shown in green. Underlined nucleotides are 2′OMe-RNA; all other nucleotides are RNA. Domain lengths: |a|=12, |b|=14, |c|=3, |y|= 2, |z|=19.

S4.2 Computational stepping analysis
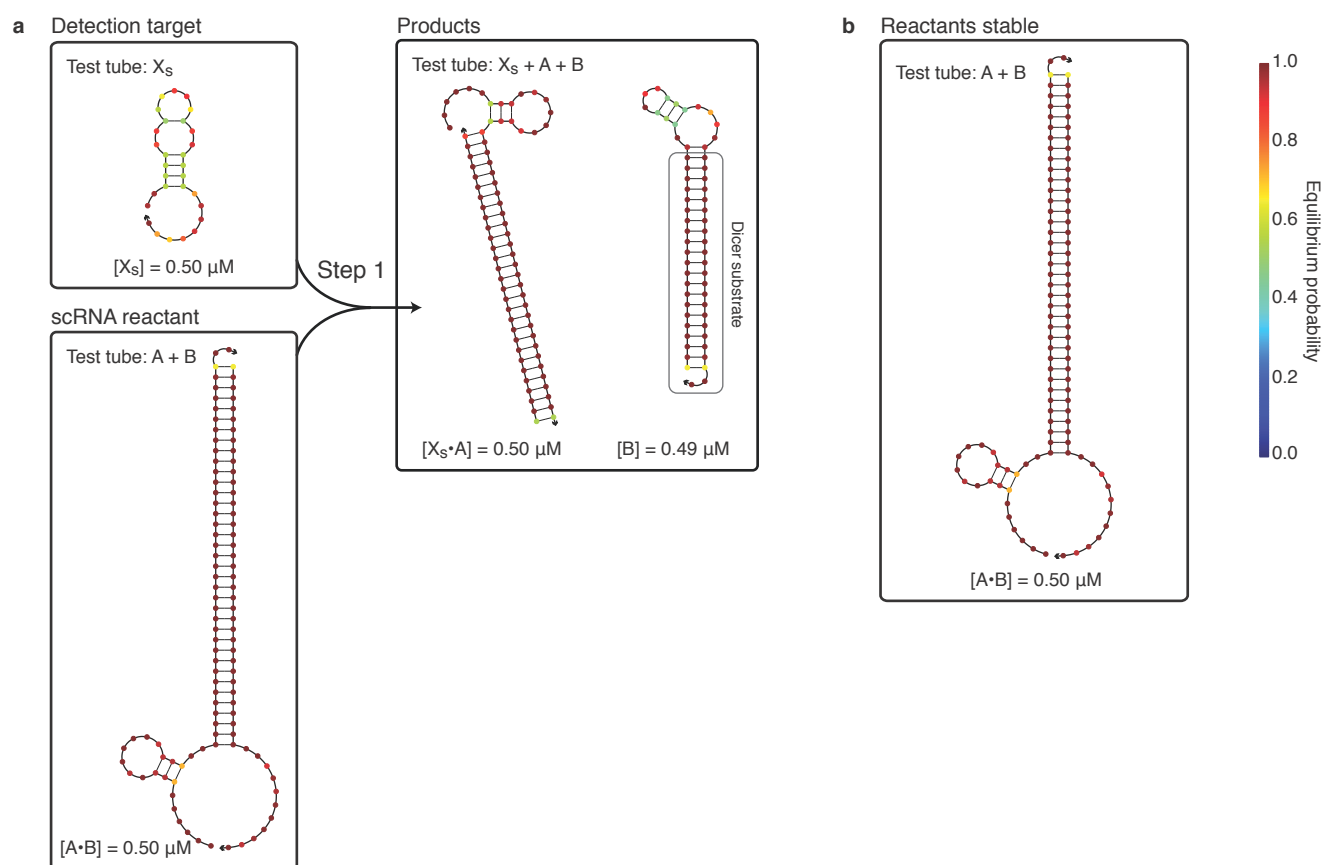
Figure S10. Computational stepping analysis for Mechanism 3. (a) Equilibrium test tube calculations showing the predicted concentrations and base-pairing properties of reactants and products. The short RNA detection target X_s is predicted to have some internal base pairing on average at equilibrium. The scRNA A·B is predicted to have some internal base pairing in a domain that is intended to be single-stranded. The reactant and products are predicted to form with near-quantitative yield. (b) Equilibrium test tube calculation predicting that scRNA A·B is stable, not metastable. Placing A and B together in a test tube leads predominantly to duplex dimer A·B at equilibrium, demonstrating that reactant A·B is stable. (a,b) Each box represents a test tube containing the strands listed at the top at 0.5 μM each. For each test tube, thermodynamic analysis at 37 °C yields the equilibrium concentrations and base-pairing ensemble properties for all complexes containing up to three strands. Each complex predicted to form with appreciable concentration at equilibrium is depicted by its minimum free energy structure, with each nucleotide shaded by the probability that it adopts the depicted base-pairing state at equilibrium. The predicted equilibrium concentration is noted below each complex.

S4.3   Mechanism stepping gel
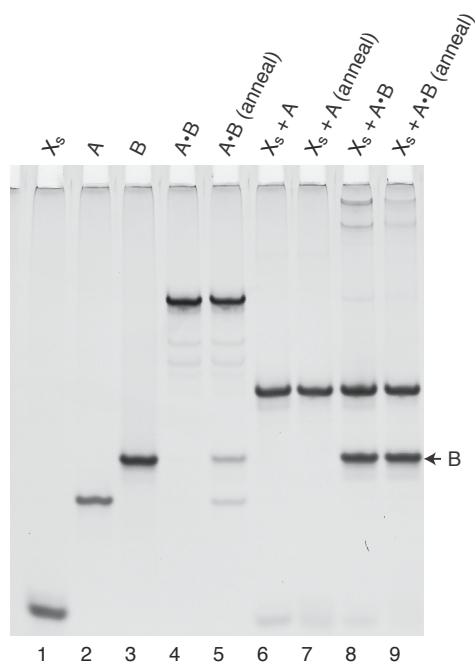
Figure S11. Stepping gel for Mechanism 3. Native PAGE demonstrating the assembly and disassembly operations in Figure 4a. Short RNA detection target: X$_s$ (lane 1). scRNA reactant: A·B (lane 4). ON state: X$_s$ and A·B interact to form products X$_s$·A and B (lane 8). OFF state: A·B yields minimal production of A and B (lane 4). Annealing A·B yields predominantly A·B, as well as some A and B (lane 5). See Section S7 for an assessment of reactant metastability vs stability.

S4.4   Dicer processing stepping gel
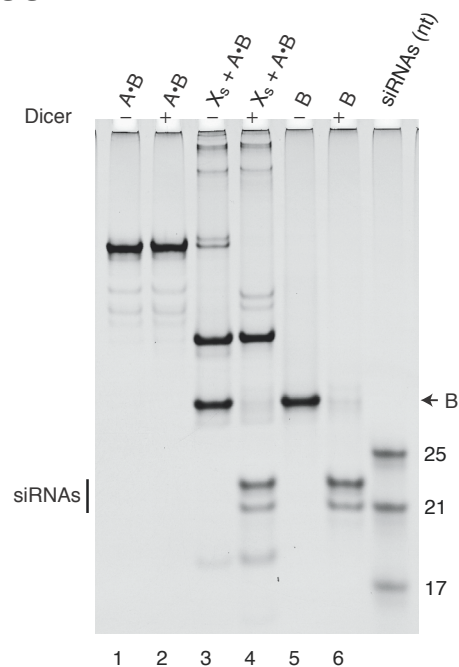
Figure S12. Dicer processing stepping gel for Mechanism 3. Native PAGE demonstrating each signal transduction step in Dicer reaction conditions in the absence/presence of Dicer (-/+ lanes). Only the final product B is efficiently processed by Dicer, yielding siRNAs (compare lanes 3 and 4).

S4.5 Quantification of conditional Dicer substrate formation
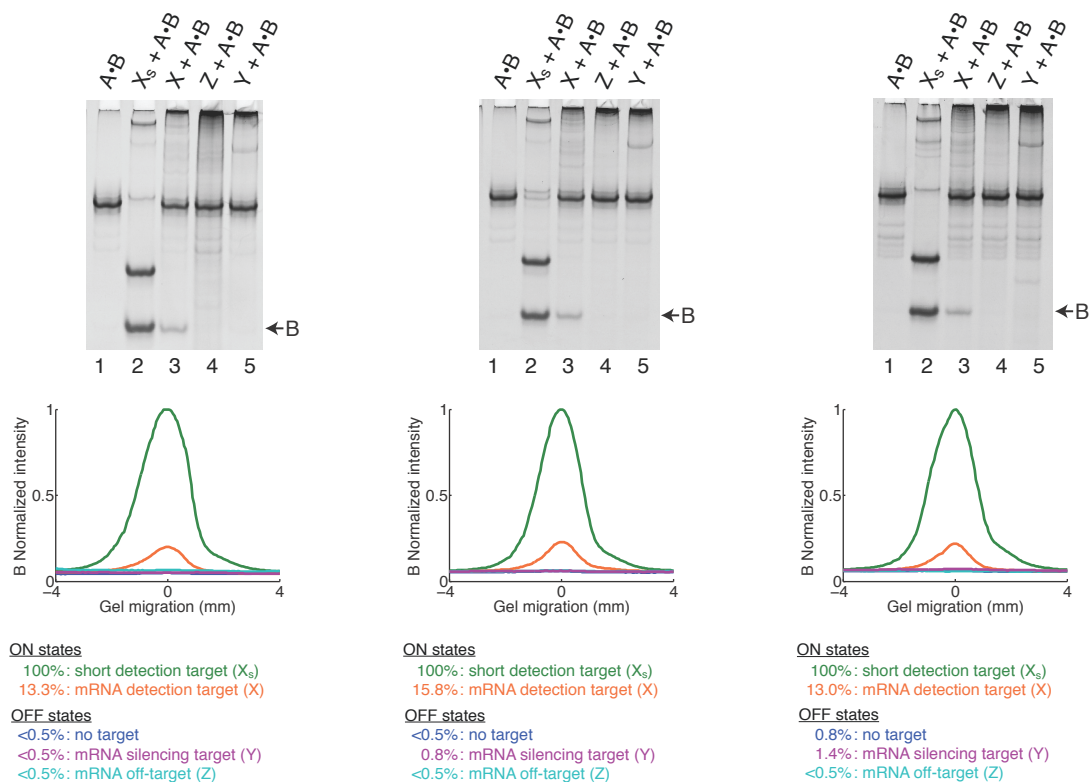
Figure S13. Quantification of conditional Dicer substrate formation for Mechanism 3. Three independent experiments were used to characterize the variability in the OFF/ON conditional response in production of Dicer substrate. OFF states: no target, mRNA silencing target Y, mRNA off-target Z. ON states: short RNA detection target X_s, mRNA detection target X. All values are normalized relative to the amount of Dicer substrate produced using X_s. A number of the OFF states were undetectable, and are denoted as $< 0.5\%$ corresponding to the estimated uncertainty in gel quantification.

S4.6 Identification of Dicer products by mass spectrometry
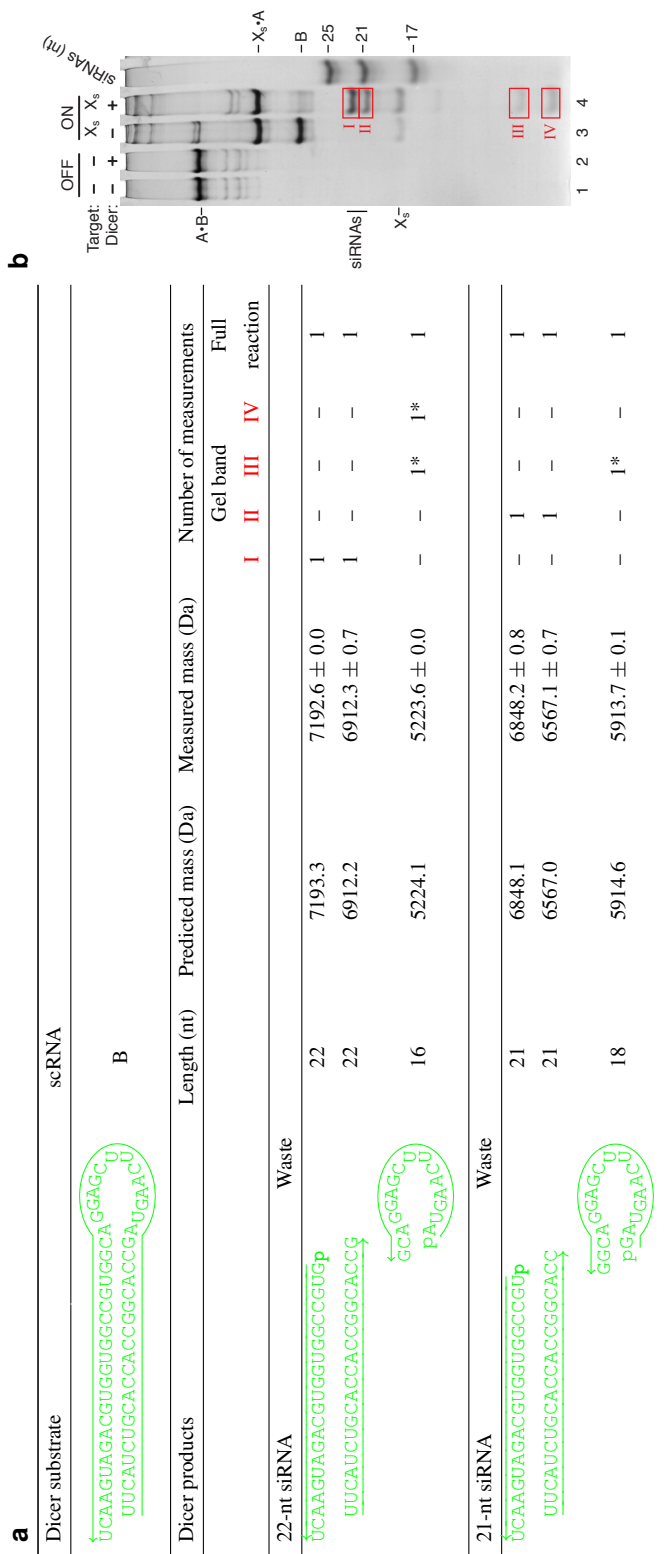
Table S7. Dicer products for Mechanism 3 identified by mass spectrometry. (a) Predicted and measured average masses for Dicer cleavage products. Canonical 21- and 22-nt siRNAs were identified, as were waste products corresponding to the loop of the shRNA. Masses were determined for specific gel bands (I, II, III, IV) and for the full reaction. For each mass, the mean and standard deviation were calculated using all measurements. 5′ phosphate group is denoted 'p' and strand polarity is indicated by an arrowhead at the 3′ end. '*' denotes gel bands cut from a lane in which only scRNA B was incubated with Dicer, as opposed to performing the full reaction in the presence of Dicer. (b) Native PAGE illustrating the approximate migration of gel bands (I, II, III, IV) that were isolated for mass spectrometry. See Supplementary Section S1.10 for methods.

S5 Mechanism 4: Conditional DsiRNA formation via template-mediated 4-way branch migration

S5.1 Sequences

Strand	Domains	Sequence
X_s	a-b-c-d-e	5′–CUCCGAGAACGUCAUCACCGAGUUCAUGCGCUUCAAGG–3′
A	e*-d*-z*-y*	5′–CCUUGAAGCGCAUGAACUGACACGCUGAACUUGUGGCCG–3′
B	y-z-b*-d	5′–CGGCCACAAGUUCAGCGUGUCUGACGUAGUUCAU–3′
C	b-z*-y*-x*	5′–ACGUCAGACACGCUGAACUUGUGGCCGUU–3′
D	x-y-z-c*-b*-a*	5′–AACGGCCACAAGUUCAGCGUGUCCGGUGAUGACGUUCUCGGAG–3′

Table S8. Sequences for Mechanism 4. Sequences constrained by DsRed2 (mRNA detection target X) are shown in red. Sequences constrained by d2EGFP (mRNA silencing target Y) are shown in green. Underlined nucleotides are 2′OMe-RNA; all other nucleotides are RNA. Domain lengths: |a|=8, |b|=6, |c|=6, |d|= 7, |e|=11, |x|=2, |y|=19, |z|=2.

S5.2 Computational stepping analysis
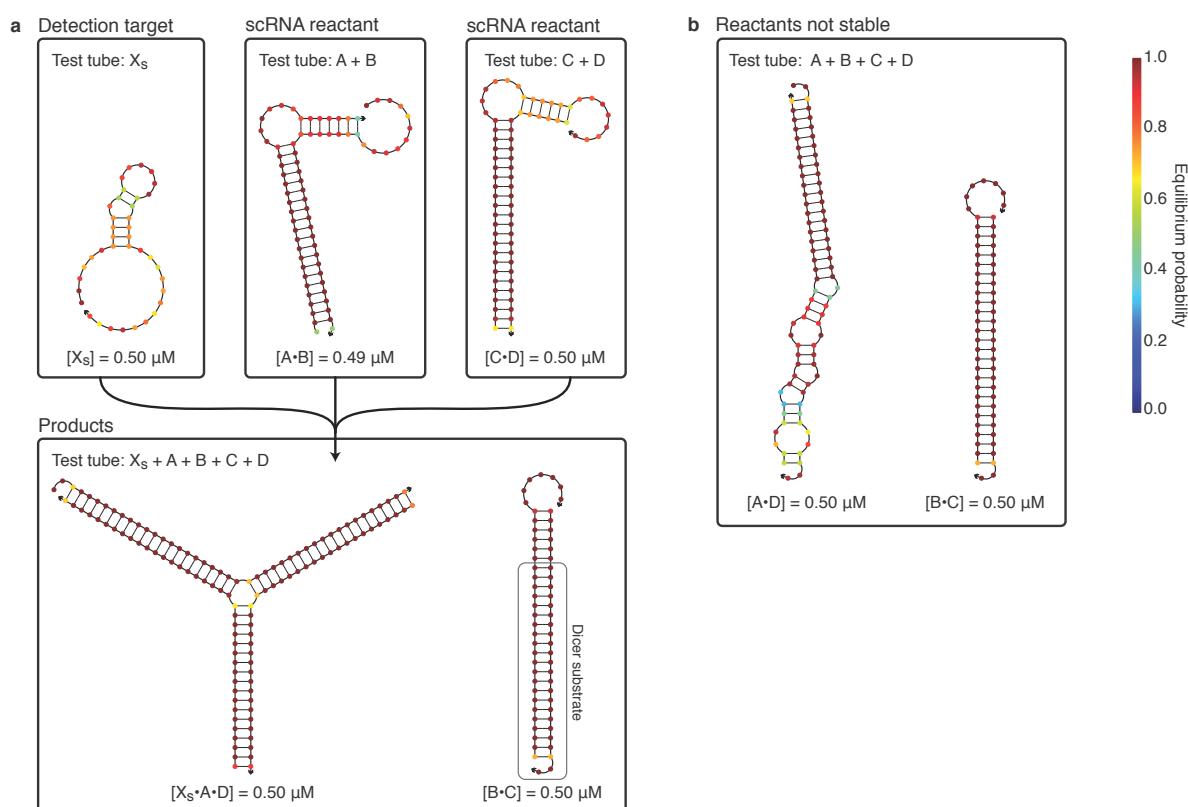
Figure S14. Computational stepping analysis for Mechanism 4. (a) Equilibrium test tube calculations showing the predicted concentrations and base-pairing properties of reactants and products. The short RNA detection target X_s is predicted to have some internal base pairing on average at equilibrium. The reactant and products are predicted to form with near-quantitative yield. (b) Equilibrium test tube calculation predicting that scRNAs A·B and C·D are metastable, not stable. Placing A, B, C, and D together in a test tube leads predominantly to duplex dimers A·D and B·C at equilibrium, demonstrating that the reactants are not stable. (a,b) Each box represents a test tube containing the strands listed at the top at 0.5 μM each. For each test tube, thermodynamic analysis at 37 °C yields the equilibrium concentrations and base-pairing ensemble properties for all complexes containing up to five strands. Each complex predicted to form with appreciable concentration at equilibrium is depicted by its minimum free energy structure, with each nucleotide shaded by the probability that it adopts the depicted base-pairing state at equilibrium. The predicted equilibrium concentration is noted below each complex.

S5.3 Mechanism stepping gel and isolation of putative pentamer intermediate
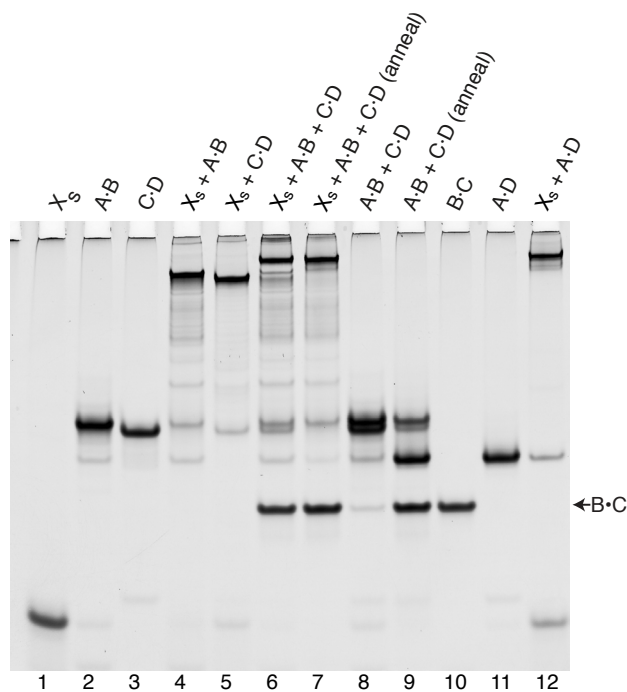
Figure S15. Stepping gel for Mechanism 4. Native PAGE demonstrating the assembly and disassembly operations in Figure 5a. Short RNA detection target: X_s (lane 1). scRNA reactants: A·B and C·D (lanes 2 and 3). Step 1 (ON state): X_s, A·B and C·D interact to form products X_s·A·D and B·C (lane 6). OFF state: A·B and C·D co-exist metastably, yielding minimal production of B·C (lane 8). Annealing A·B and C·D leads to substantial production of B·C (lane 9). See Section S7 for an assessment of reactant metastability vs stability.
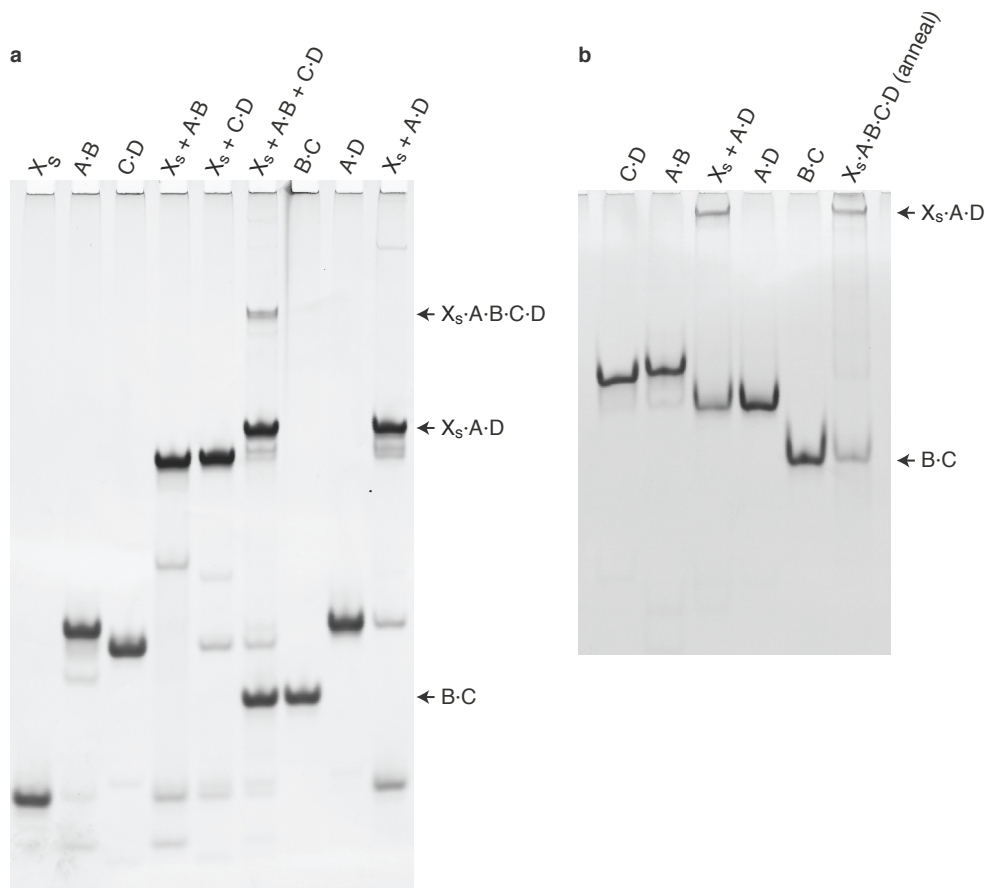
Figure S16. Isolation of putative pentamer intermediate for Mechanism 4. (a) 10% native PAGE showing that the full reaction, X_s + A·B + C·D, leads to formation of a putative pentamer intermediate band, X_s·A·B·C·D. (b) 20% native PAGE showing that the putative pentamer intermediate, X_s·A·B·C·D, when isolated from a native gel and annealed, dissociates into the final products X_s·A·D, and B·C, indicating that all five strands are present in the complex. To purify the putative pentamer, the full reaction, X_s + A·B + C·D, was scaled to 150 μL (standard 2 h at 37 °C with 0.5 μM reactants) and separated by 10% native PAGE with SYBR Gold (Life Technologies, catalog #S-11494) post-staining. The putative pentamer band was visualized with a UV transilluminator and excised from the gel. The gel slice was crushed with a Zymo Squisher (Zymo, catalog # H1001) and the nucleic acids were eluted by soaking in 0.3 M sodium acetate overnight with gentle rotation. The nucleic acids were purified by ethanol precipitation, followed by a Zymo Oligo Clean and Concentrator column (Zymo, catalog #D4060). The nucleic acids isolated from the putative pentamer band were annealed and separated by 20% native PAGE as shown in panel (b).

S5.4 Dicer processing stepping gel
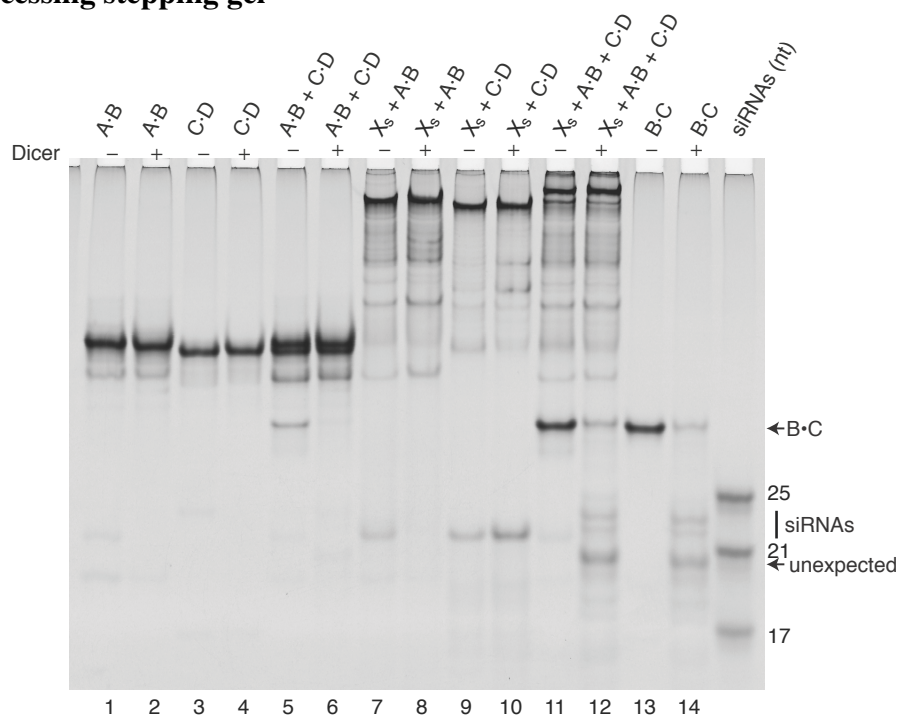
Figure S17. Dicer processing stepping gel for Mechanism 4. Native PAGE demonstrating each signal transduction step in Dicer reaction conditions in the absence/presence of Dicer (-/+ lanes). Only the final product B·C is efficiently processed by Dicer, yielding siRNAs and some unexpected Dicer products (compare lanes 11 and 12).

S5.5 Quantification of conditional Dicer substrate formation
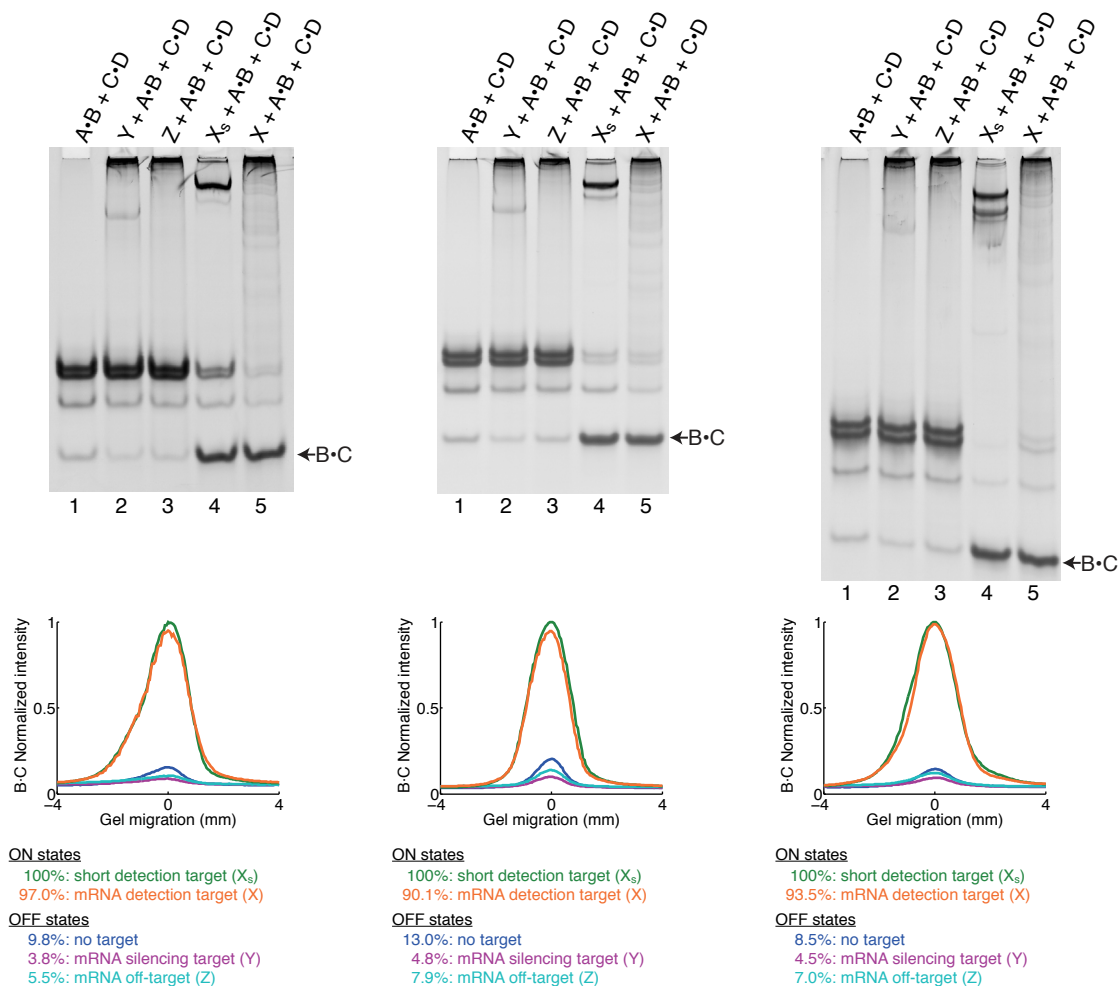
Figure S18. Quantification of conditional Dicer substrate formation for Mechanism 4. Three independent experiments were used to characterize the variability in the OFF/ON conditional response in production of Dicer substrate. OFF states: no target, mRNA silencing target Y, mRNA off-target Z. ON states: short RNA detection target X_s, mRNA detection target X. All values are normalized relative to the amount of Dicer substrate produced using X_s.

S5.6 Identification of Dicer products by mass spectrometry

a

Dicer substrate	scRNA
UUGCCGGUGUUCAAGUCGCACAGACUGCA	C
CGGCCACAAGUUCAGCGUGUCUGACGUAGUUCAU	B

b

Dicer products	Length (nt)	Predicted mass (Da)	Measured mass (Da)	Gel band I	Gel band II	Full reaction
24-nt siRNA						
UUGCCGGUGUUCAAGUCGCACAGAp	24	7745.005	7744.999 ± 0.001	1	–	1
CGGCCACAAGUUCAGCGUGUCUGA	24	7664.054	7664.051 ± 0.001	1	–	1
23-nt siRNA Waste						
UUGCCGGUGUUCAAGUCGCACAGp	23	7415.952	7415.951 ± 0.005	1	1	1
CGGCCACAAGUUCAGCGUGUCUG	23	7335.002	7335.001 ± 0.003	1	1	1
pACGUAGUUCAU	11	3529.447	3529.447	–	–	1
22-nt siRNA Waste						
UUGCCGGUGUUCAAGUCGCACAp	22	7070.905	7070.912 ± 0.005	1	1	1
CGGCCACAAGUUCAGCGUGUCU	22	6989.955	6989.960 ± 0.008	1	1	1
pGACGUAGUUCAU	12	3874.494	3874.494	–	–	1
21-nt siRNA Waste						
UUGCCGGUGUUCAAGUCGCACp	21	6741.852	6741.855 ± 0.007	1	1	1
CGGCCACAAGUUCAGCGUGUC	21	6683.929	6683.929 ± 0.005	1	1	1
pUGACGUAGUUCAU	13	4180.520	4180.522	–	–	1
21-nt siRNA trimmed from 23-nt siRNA Waste						
GCCGGUGUUCAAGUCGCACAGp	21	6803.902	6803.896 ± 0.003	1	1	1
pGCCACAAGUUCAGCGUGUCUG	21	6764.880	6764.881 ± 0.006	1	1	1
pACGUAGUUCAU	11	3529.447	3529.447	–	–	1
13-nt Unexpected						
UUGCCGGUGUUCAp	13	4172.503	4172.504 ± 0.002	1	–	1
CGGCCACAAGUUC	13	4097.601	4097.601	–	–	1
AGUCGCACAGACUGCA	16	5100.754	5100.753 ± 0.002	–	1	1
pAGCGUGUCUGACGUAGUUCAU	21	6766.848	6766.863 ± 0.012	–	1	1
12-nt Unexpected						
UUGCCGGUGUUCp	12	3843.451	3843.452 ± 0.004	1	–	1
CGGCCACAAGUU	12	3792.560	3792.562	–	–	1
AAGUCGCACAGACUGCA	17	5429.806	5429.811 ± 0.006	1	1	1
pCAGCGUGUCUGACGUAGUUCAU	22	7071.889	7071.908 ± 0.006	–	1	1
11-nt Unexpected						
UUGCCGGUGUUp	11	3538.409	3538.410	–	–	1
CGGCCACAAGU	11	3486.535	3486.533	–	–	1
CAAGUCGCACAGACUGCA	18	5734.847	5734.850 ± 0.004	1	1	1
pUCAGCGUGUCUGACGUAGUUCAU	23	7377.914	7377.916 ± 0.007	1	1	1
10-nt Unexpected						
UUGCCGGUGUp	10	3232.384	3232.384	–	–	1
CGGCCACAAG	10	3180.509	3180.506	–	–	1
UCAAGUCGCACAGACUGCA	19	6040.873	6040.876 ± 0.001	1	–	1
pUUCAGCGUGUCUGACGUAGUUCAU	24	7683.939	7683.944 ± 0.003	1	1	1
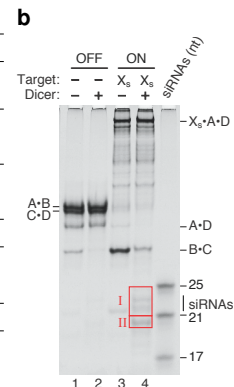
Table S9. Dicer products for Mechanism 4 identified by high resolution mass spectrometry. (a) Predicted and measured monoisotopic masses for Dicer cleavage products. Canonical 21–24-nt siRNAs were identified, as were waste products corresponding to the non-siRNA portion of the substrate (only the waste from strand B was identified as the waste from strand C was too short to be retained during sample purification). Additional Dicer products are produced by unexpected cleavage of the Dicer substrate within domains 'y' and 'y*', suggesting that for some fraction of the substrates, Dicer is either measuring unusually short siRNAs (10–13-nt) from the cognate end of the substrate (which has a canonical 2-nt 3′-overhang), or is measuring from the non-cognate end of the substrate (which has a 7-nt 3′-overhang). Masses were determined for specific sets of gel bands (I, II) and for the full reaction. For each mass, the mean and standard deviation were calculated using all measurements. Only Dicer cleavage products where one duplex was identified at least twice are tabulated. 5′ phosphate group is denoted 'p' and strand polarity is indicated by an arrowhead at the 3′ end. (b) Native PAGE illustrating the approximate migration of specific sets of gel bands (I, II) that were isolated for mass spectrometry. Additional studies with ESI-TOF LC-MS indicate that set I is predominantly canonical 21–24-nt siRNAs and set II is predominantly unexpected cleavage products. See Supplementary Section S1.10 for methods.

S6 Mechanism 5: Conditional shRNA transcription using scDNAs

S6.1 Sequences

Strand	Domains	Sequence
X$_s$	a-b	5′-ATAAGCCCTCATCCAACT-3′
A	b*-a*-p-q-z-y*-z*-q*-a	5′-AGTTGGATGAGGGCTTATtaatacgactcactatagCAGCACGACTTCTTCAAGAGCTGACTTGAAGAA GTCGTGCTGCtatagtgagATAAGCCCTC-3′
B	q-t-z-y-z*-q*-p*	5′-ctcactataAAAAAAAGCAGCACGACTTCTTCAAGTCAGCTCTTGAAGAAGTCGTGCTGCtatagtgag tcgtatta-3′
C	z-y*-z*-poly(U)	5′-gCAGCACGACUUCUUCAAGAGCUGACUUGAAGAAGUCGUGCUGCpoly(U)-3′

Table S10. Sequences for Mechanism 5. Sequences constrained by d2EGFP (mRNA silencing target Y) are shown in green. Sequences constrained by the T7 promoter are shown as lower case letters. Sequences constrained by the T7 transcription termination sequence are shown in blue. Unconstrained sequences are shown as upper case black letters. X$_s$, A, and B are DNA; C is an shRNA in vitro transcription product. The terminal poly(U) in shRNA C results from the transcription termination sequence. Domain lengths: |a|=10, |b|=8, |p|=8, |q|= 9, |t|=7, |y|=6, |z|=19.

S6.2 Computational stepping analysis
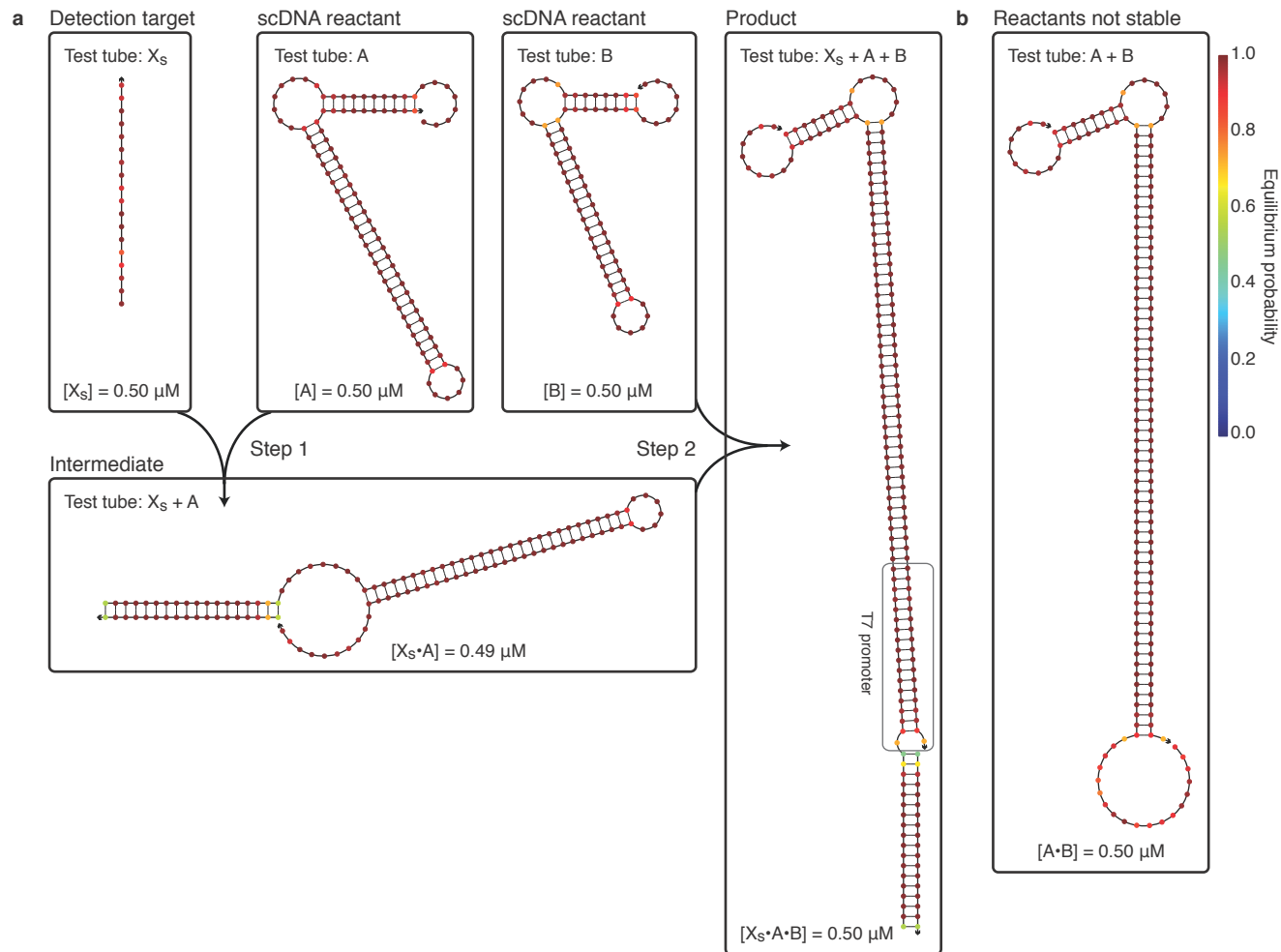
Figure S19. Computational stepping analysis for Mechanism 5. (a) Equilibrium test tube calculations showing the predicted concentrations and base-pairing properties of reactants, intermediates, and products. Reactants, intermediates, and products are predicted to form with near-quantitative yield. (b) Equilibrium test tube calculation predicting that scDNAs A and B are metastable, not stable. Placing A and B together in a test tube leads predominantly to duplex dimer A·B at equilibrium,

demonstrating that A and B are not stable. (a,b) Each box represents a test tube containing the strands listed at the top at 0.5 μM each. For each test tube, thermodynamic analysis at 37 °C yields the equilibrium concentrations and base-pairing ensemble properties for all complexes containing up to three strands. Each complex predicted to form with appreciable concentration at equilibrium is depicted by its minimum free energy structure, with each nucleotide shaded by the probability that it adopts the depicted base-pairing state at equilibrium. The predicted equilibrium concentration is noted below each complex.

S6.3 Mechanism stepping gel
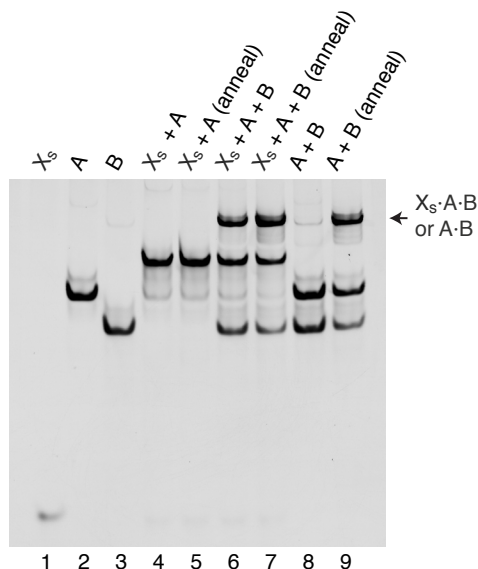
Figure S20. Stepping gel for Mechanism 5. Native PAGE demonstrating the assembly operations in Figure 6a. Short DNA detection target: X_s (lane 1). scDNA reactants: A and B (lanes 2 and 3). Step 1: X_s and A interact to form intermediate $X_s \cdot A$ (lane 4). Step 1 + Step 2 (ON state): X_s, A and B interact to form product $X_s \cdot A \cdot B$ (lane 6). OFF state: A and B co-exist metastably, yielding minimal production of A·B (lane 8). Annealing A and B leads to substantial production of A·B (lane 9). See Section S7 for an assessment of reactant metastability vs stability.

S6.4 Transcription and Dicer processing stepping gel
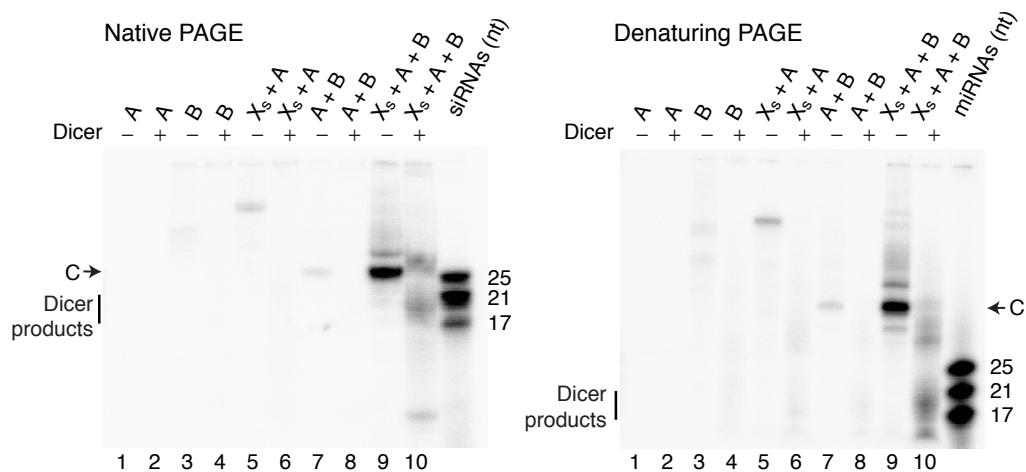
Figure S21. Transcription and Dicer processing stepping gel for Mechanism 5. Native and denaturing PAGE demonstrating each signal transduction step. In vitro transcription is performed concurrently with scDNA signal transduction. Optional Dicer processing is performed following in vitro transcription (-/+ lanes). Step 1: Minimal transcription is observed for a product that is longer than the expected shRNA C (lane 5). OFF state: Minimal transcription of shRNA C (lane 7). Step 1 + Step 2 (ON state): Substantial transcription of shRNA C (lane 9), which is efficiently processed by Dicer (lane 10). Each reaction was split in half and separated by either 20% native PAGE (250 V for 4 h) or 15% denaturing PAGE (500 V for 1.5 h).

S6.5 Quantification of conditional Dicer substrate transcription
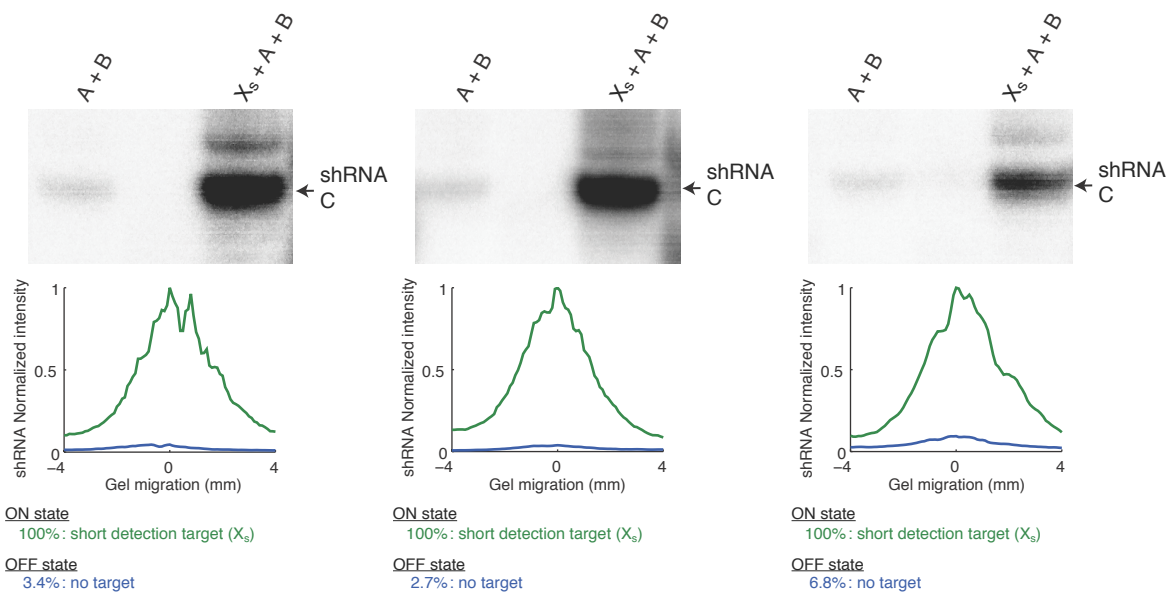
Figure S22. Quantification of conditional Dicer substrate transcription for Mechanism 5. Three independent experiments were used to characterize the variability in the OFF/ON conditional response in production of Dicer substrate. OFF state: no target. ON state: short DNA detection target X_s. All values are normalized relative to the amount of Dicer substrate produced using X_s.

S6.6 Identification of Dicer products by mass spectrometry

Mass spectrometry revealed that the dominant transcription product is a 51-nt shRNA with a 19-bp stem and a non-canonical 7-nt poly(U) 3′-overhang; shRNAs with shorter poly(U) tails were transcribed in lesser amounts. Mass spectrometry of Dicer-processed transcription reactions identified products that correspond to either one or two cuts of the hairpin stem (Supplementary Table S11). Hairpins cut in two places produced short duplexes with a canonical 2-nt 3′-overhang at one end. Canonical siRNAs were not identified for this Dicer substrate. Mass spectrometry of a synthetic shRNA with a 19-bp stem and a canonical 2-nt 3′-overhang was cleaved similarly, yielding short siRNA-like duplexes with canonical 2-nt 3′-overhangs at both ends. Again, canonical siRNAs were not observed, suggesting that the failure to observe canonical siRNAs for the transcription products of Mechanism 5 results from the short 19-bp stem. shRNAs with a 19-bp stem and canonical 2-nt 3′-overhang are known to be potent silencers[12–14] but it has been observed that these short shRNAs are not substrates for Dicer.[12,13] The current design for Mechanism 5 yields shRNAs with a 19-bp stem that are expected to mediate silencing, but are not well-suited for production of canonical siRNAs. Future designs could employ a longer stem (e.g., the 22-bp stem of Mechanism 3 was processed by Dicer into canonical siRNAs).

Dicer substrate	scRNA			
UUUUUUUCGUCGUGCUGAAGAAGUUC A G U / pppGCAGCACGACUUCUUCAAG A G C (hairpin)	C			

Dicer products	Length (nt)	Predicted mass (Da)	Measured mass (Da)	Number of measurements
14-nt Waste				
UUUUUUUCGUCGUGCUGAAp	19	6031.682	6031.691 ± 0.004	2
pppGCAGCACGACUUCU	14	4643.525	4643.529 ± 0.003	2
GAAGUUC A G U / pUCAAG A G C (hairpin)	18	5856.788	5856.789 ± 0.006	2
GAAGUUC A G U / pppGCAGCACGACUUCUUCAAG A G C (hairpin)	32	10482.303	10482.313 ± 0.003	2
UUUUUUUCGUCGUGCUGAAGAAGUUC A G U / pUCAAG A G C (hairpin)	37	11870.459	11870.465 ± 0.003	2
15-nt Waste				
UUUUUUUCGUCGUGCUGAAGp	20	6376.730	6376.734 ± 0.006	2
pppGCAGCACGACUUCUU	15	4949.551	4949.554 ± 0.004	2
AAGUUC A G U / pCAAG A G C (hairpin)	16	5205.715	5205.714 ± 0.002	2
AAGUUC A G U / pppGCAGCACGACUUCUUCAAG A G C (hairpin)	31	10137.255	10137.268 ± 0.001	2
UUUUUUUCGUCGUGCUGAAGAAGUUC A G U / pCAAG A G C (hairpin)	36	11564.434	11564.426 ± 0.002	2

Table S11. Dicer products for Mechanism 5 identified by high resolution mass spectrometry. Predicted and measured monoisotopic masses for Dicer cleavage products from a transcribed 51-nt shRNA with a 19-bp stem and a non-canonical 7-nt 3′-overhang. Identified products correspond to either one or two cuts of the hairpin stem. Hairpins cut in two places produced short duplexes with canonical 2-nt 3′-overhang at one end. Canonical siRNAs were not identified for this Dicer substrate. Similar cleavage patterns were observed for transcribed hairpins with shorter poly(U) 3′-overhangs. For each mass, the mean and standard deviation were calculated using all measurements. 5′ triphosphate is denoted 'ppp', 5′ phosphate is denoted 'p', and strand polarity is indicated by an arrowhead at the 3′ end. See Supplementary Section S1.10 for methods.

Dicer substrate	scRNA			
UUCGUCGUGCUGAAGAAGUUC A G U / GCAGCACGACUUCUUCAAG A G C (hairpin)	C			

Dicer products	Length (nt)	Predicted mass (Da)	Measured mass (Da)	Number of measurements
14-nt Waste				
UUCGUCGUGCUGAAp	14	4503.6	4502.8 ± 0.0	2
GCAGCACGACUUCU	14	4405.7	4405.6 ± 0.0	2
GAAGUUC A G U / pUCAAG A G C (hairpin)	18	5859.5	5859.2 ± 0.0	2
GAAGUUC A G U / GCAGCACGACUUCUUCAAG A G C (hairpin)	32	10247.0	10245.4 ± 0.3	2
UUCGUCGUGCUGAAGAAGUUC A G U / pUCAAG A G C (hairpin)	32	10345.0	10344.4 ± 0.6	2
15-nt Waste				
UUCGUCGUGCUGAAGp	15	4848.8	4848.0 ± 0.0	2
GCAGCACGACUUCUU	15	4711.9	4711.7 ± 0.1	2
AAGUUC A G U / pCAAG A G C (hairpin)	16	5208.1	5207.8 ± 0.3	2
AAGUUC A G U / GCAGCACGACUUCUUCAAG A G C (hairpin)	31	9902.0	9900.8 ± 0.6	2
UUCGUCGUGCUGAAGAAGUUC A G U / pCAAG A G C (hairpin)	31	10039.0	10038.2 ± 0.3	2
21-nt Waste				
UUCGUCGUGCUGAAGAAGUUCp	21	6770.0	6769.7 ± 0.1	2
A G U / GCAGCACGACUUCUUCAAG A G C (hairpin)	25	7980.9	7979.8 ± 0.3	2

Table S12. Dicer products for a synthetic shRNA identified by mass spectrometry. Predicted and measured average masses for Dicer cleavage products from a synthetic 46-nt shRNA with a 19-bp stem and a canonical 2-nt 3′-overhang. Identified products correspond to either one or two cuts of the hairpin stem. Hairpins cut in two places produced short siRNA-like duplexes with canonical 2-nt 3′-overhangs at both ends. Canonical siRNAs were not identified for this Dicer substrate. For each mass, the mean and standard deviation were calculated using all measurements. 5′ phosphate group is denoted 'p' and strand polarity is indicated by an arrowhead at the 3′ end. See Supplementary Section S1.10 for methods.

S7 Reactant metastability vs stability

In classifying the design principles underlying each mechanism, a major distinguishing feature is reactant metastability vs reactant stability. Metastable reactants are kinetically trapped. If they are allowed to equilibrate in the absence of the detection target, they will form the transduction product even in the absence of the detection target. In order to obtain a clean OFF/ON conditional response using metastable scRNAs or scDNAs, it is important that they 'leak' out of the kinetically trapped state slowly. On the other hand, if stable reactants are allowed to equilibrate in the absence of the detection target, they will predominantly remain in the reactant state rather than converting to the product state. This is a major conceptual advantage because it places a thermodynamic rather than a kinetic limit on the amount of spurious transduction product that can form in the absence of the detection target.

To examine whether scRNA (or scDNA) reactants are predicted to be stable in the absence of the detection target, we used the Analysis page of the NUPACK web application[1] to perform a computational thermodynamic analysis for a test tube containing all the reactants for a given mechanism (see Sections S2.2, S3.2, S4.2, S5.2, S6.2); the results are summarized in Table S13. For Mechanisms 1, 4, and 5, full conversion to product is observed whether or not short detection target X_s is present, indicating that these reactants are predicted not to be stable. In order to achieve clean OFF/ON signal transduction, these mechanisms must rely on reactant metastability (which cannot be assessed via these equilibrium calculations). For Mechanisms 2 and 3, minimal conversion to product is observed at equilibrium in the absence of X_s, indicating that these reactants are predicted to be stable.

	Reactants only		Reactants + X_s		Computational	Experimental
Mechanism	Product	Concentration (μM)	Product	Concentration (μM)	classification	classification
1	B·C	0.5	B·C	0.5	not stable	metastable
2	B·C	1×10^{-3}	B·C	0.5	stable	stable
3	B	2×10^{-7}	B	0.5	stable	stable
4	B·C	0.5	B·C	0.5	not stable	metastable
5	A·B	0.5	X_s·A·B	0.5	not stable	metastable

Table S13. Computational and experimental classification of reactant metastability vs stability. For each mechanism, computational thermodynamic analysis is performed for a test tube at 37 °C containing all scRNA (or scDNA) reactants in the absence or presence of short detection target X_s (each strand at 0.5 μM). For experimental classification, see below.

Experimental studies confirm that the reactants for Mechanisms 1, 4, and 5 are metastable and that the reactants for Mechanisms 2 and 3 are stable:

- **Mechanism 1 (metastable reactants):** Catalytic formation of Dicer substrate B·C (Fig. 2 and Fig. S5) demonstrates that equilibrium partitioning between reactants B and C and product B·C strongly favors product formation. Hence, that fact that scRNA reactants A, B and C co-exist for 2 h at 37 °C with only minimal production of Dicer substrate B·C demonstrates metastability (Fig. 2 (lane 1) and Fig. S2 (lane 11)). Annealing A, B, C yields increased production of B·C (Fig. S2 (lane 12)), but the reactant state is still favored, consistent with the annealing properties of metastable hairpins (see Section S1.9).

- **Mechanism 2 (stable reactants):** scRNA reactants A·B and C co-exist for 2 h at 37 °C with only minimal production of A and B·C (Fig. 3 (lane 1) and Fig. S7 (lane 15)). Annealing A·B and C yields only slightly increased production of A and B·C (Fig. S7 (lane 16)). Because of the annealing properties of hairpins (see Section S1.9), the anneal is expected to favor the reactant state of C, so these results do not provide definitive evidence of reactant stability. To establish that the reactants are in fact stable and not metastable, we monitored the reverse reaction (A + B·C → A·B + C) using a time course experiment (Fig. S23). To account for possible stoichiometry mismatches between the initial species, we performed the experiment with either A as the limiting reagent or with B·C as the limiting reagent. In both cases, the reverse reaction proceeded until the limiting reagent was predominantly consumed, demonstrating that the scRNAs A·B and C are stable, not metastable.

- **Mechanism 3 (stable reactants):** scRNA reactant A·B yields no detectible production of A and B after 2 h at 37 °C (Fig. 4 (lane 1) and Fig. S11 (lane 4)). Annealing A·B yields increased but minimal production of

A and B (Fig. S11 (lane 5)). Because of the annealing properties of hairpins (see Section S1.9), the anneal is expected to favor the product state of B. Hence, these results are consistent with stability of the scRNA reactants and may actually overestimate the equilibrium concentration of the product state. To confirm that the reactants are stable, we monitored the reverse reaction (A + B → A·B) using a time course experiment (Fig. S24). To account for possible stoichiometry mismatches between the initial species, we performed the experiment with either A as the limiting reagent or with B as the limiting reagent. In both cases, the reverse reaction proceeded until the limiting reagent was predominantly consumed, demonstrating that the scRNA A·B is stable, not metastable.

- **Mechanism 4 (metastable reactants):** scRNA reactants A·B and C·D co-exist for 2 h at 37 °C with minimal production of Dicer substrate B·C (Fig. 5 (lane 1) and Fig. S15 (lane 8)). Annealing A·B and C·D yields substantial production of A·D and B·C (Fig. S15 (lane 9)). This anneal is not expected to favor either reactants or products, as none of the strands are expected to have substantial internal secondary structure (see Section S1.9). Hence, the anneal strongly suggests that the reactants are metastable, not stable.

- **Mechanism 5 (metastable reactants):** scDNA reactants A and B co-exist for 2 h at 37 °C with minimal production of transcription template A·B (Fig. 6b (lane 1) and Fig. S20 (lane 8)). Annealing A and B yields substantial production of A·B (Fig. S20 (lane 9)). This anneal is expected to favor reactants over products, because A and B are both hairpins (see Section S1.9). Hence, the fact that the anneal nonetheless produces a substantial quantity of A·B strongly suggests that the reactants are metastable, not stable.
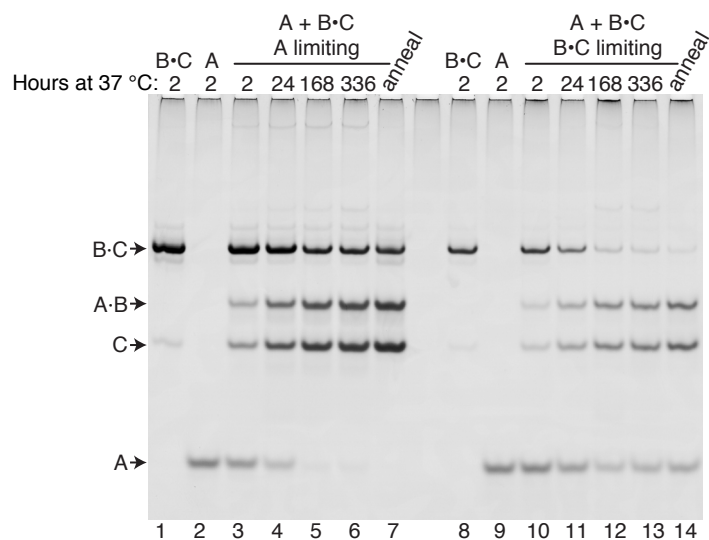
Figure S23. Demonstrating scRNA stability for Mechanism 2. Native PAGE demonstrating that the reverse reaction A + B·C → A·B + C nearly exhausts the limiting reagent with either A or B·C limiting. Incubation at 37 °C for 2, 24, 168 (1 week), or 336 (2 weeks) h.
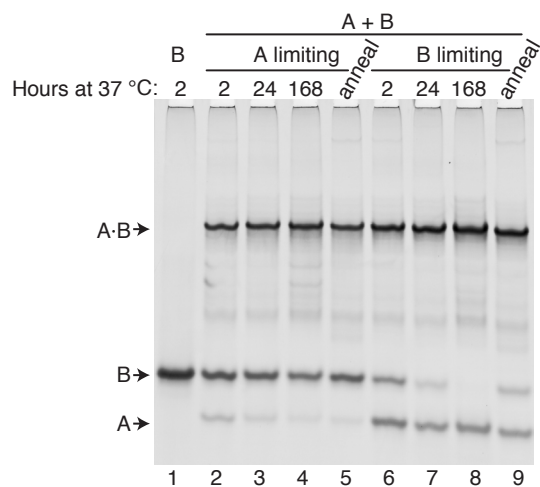
Figure S24. Demonstrating scRNA stability for Mechanism 3. Native PAGE demonstrating that the reverse reaction A + B → A·B nearly exhausts the limiting reagent with either A or B limiting. Incubation at 37 °C for 2, 24, or 168 (1 week) h.

References

[1] Zadeh, J. N.; Steenberg, C. D.; Bois, J. S.; Wolfe, B. R.; Pierce, M. B.; Khan, A. R.; Dirks, R. M.; Pierce, N. A. *J. Comput. Chem.* **2011**, 32, 170–173.

[2] Dirks, R. M.; Lin, M.; Winfree, E.; Pierce, N. A. *Nucleic Acids Res.* **2004**, 32, 1392–1403.

[3] Zadeh, J. N.; Wolfe, B. R.; Pierce, N. A. *J. Comput. Chem.* **2011**, 32, 439–452.

[4] Serra, M. J.; Turner, D. H. *Methods Enzymol.* **1995**, 259, 242–261.

[5] SantaLucia, J., Jr. *Proc. Natl. Acad. Sci. U. S. A.* **1998**, 95, 1460–1465.

[6] Feldkamp, U.; Niemeyer, C. M. *Angew. Chem., Int. Ed.* **2006**, 45, 1856–1876.

[7] Bois, J. S., *Analysis of interacting nucleic acids in dilute solutions*. Ph.D. Thesis, California Institute of Technology, **2007**.

[8] Yin, P.; Choi, H. M. T.; Calvert, C. R.; Pierce, N. A. *Nature* **2008**, 451, 318–322.

[9] Jinek, M.; Doudna, J. A. *Nature* **2009**, 457, 405–412.

[10] Du, Q. A.; Thonberg, H.; Wang, J.; Wahlestedt, C.; Liang, Z. C. *Nucleic Acids Res.* **2005**, 33, 3698–3698.

[11] Lima, W. F.; Wu, H. J.; Nichols, J. G.; Sun, H.; Murray, H. M.; Crooke, S. T. *J. Biol. Chem.* **2009**, 284, 26017–26028.

[12] Siolas, D.; Lerner, C.; Burchard, J.; Ge, W.; Linsley, P. S.; Paddison, P. J.; Hannon, G. J.; Cleary, M. A. *Nat. Biotechnol.* **2005**, 23, 227–231.

[13] Ge, Q.; Ilves, H.; Dallas, A.; Kumar, P.; Shorenstein, J.; Kazakov, S. A.; Johnston, B. H. *RNA* **2010**, 16, 106–117.

[14] Mcintyre, G. J.; Yu, Y. H.; Lomas, M.; Fanning, G. C. *BMC Mol. Biol.* **2011**, 12, 34.